Mohamed Khider University of Biskra
Faculty of exact sciences and natural and life sciences
Material sciences department

MASTER MEMORY

Material sciences
Physics
Condensed matter physics

Prsentedd by:
Saihi Manel
on :04/06/2024

THE EFFECT OF LITHIUM DOPING ON THE PROPERTIES OF TITANIUM DIOXIDE THIN FILMS ELABORATED BY SOL-GEL (SPIN COATING).

Jury:

Mrs. Marmi Saida	MCA	University of Biskra	President
Mrs. Saidi Hanane	Pr	University of Biskra	Supervisor
Mrs. Hamani Nadjette	MCB	University of Biskra	Examiner

AcademicYear : 2023/2024

{يَرْفَعِ اللَّهُ الَّذِينَ آمَنُوا مِنْكُمْ وَالَّذِينَ أُوتُوا الْعِلْمَ دَرَجَاتٍ}

[المجادلة: ١١]

إهداء

قبل كل شيء و بعد كل شيء احمد الله عز وجل على توفيقه لوصولي لهاته المرحلة وإكتسابي لهذا الكم المتواضع من العلم.

احمد الله على كوني خلقا من عباده المسلمين،الذين يسعون لنيل رضاه و رضا الوالدين و اتباع كل سبل العلم.

احمد الله لكوني ابنةً لأم تحمل كل معاني الحب و إبنةً لأب يحمل كل سمات المسؤولية.

احمد الله كوني حفيدة قلب لا تعرف سوى الحنان ،وحفيدة روح فارقنا كان ولا يزال في الاذهان.

احمد الله كوني اختا بين اربع إخوة جعلنا الله كتماسك اصابع اليد الواحدة.

فلي اختا ان غاب عنا الضوء اوقدت روحها نورا,و لي اخ ان غاب الأمان وقف شامخا فوق الردام و لي اختين صغيرتين ان غابتا غابت البهجة حولنا, **فريال**, **زين العابدين**, **ميار** و**رهف**, حفظهم الله.

وفي الاخير احمد الله على كوني ضمن أجمل دفعتة, فيزياء المادة المكثفة **شيماء , جمانة, كوثر , اصيل, احمد** وميزها كل من زملاء مدرسين علمونا معنى الثبات و الإرادة الأستاذ **هياق, ثابت** و**إبراهيم**.

وصديقاتي رفيقات شبابي التي لم ولن اندم عليهن ابدا **يسرى** و**هديل** دمتم لي يا غاليات.

Acknowledgment

After a long journey filled with seriousness and diligence, I am delighted to express my sincere thanks and gratitude to all those who contributed to completing this thesis.

I want to extend my utmost gratitude and appreciation to my supervisor Mrs. **Saidi Hanane**, *for their continuous support, valuable guidance, and endless patience throughout preparing this thesis. Their guidance and academic support have significantly impacted bringing this work to fruition.*

I would also like to thank the members of the examination committee Mrs. **Marmi Saida** *and* Mrs **Hamani Nadjette**, *for their constructive feedback and valuable suggestions that have contributed to improving the quality of this work.*

*I want to express my sincere gratitude for Mr.**Attaf Abdallah's** support and attention in ensuring the completion of my work to the highest standard. His guidance and dedication have been invaluable.*

*Also, I extend my sincere thanks to the Ph.D students **Okba Ben Khetta,Ranida Bourhefir** , **Nour el houda**,**Amina yousef ,** and the student **Heribi Ouissal** especially those in the Thin Section Laboratory for their contribution to the completion of this thesis. Many thanks to all of you, and may God bless you with every goodness.*

*Finally I thank all my professors and colleagues at the **University of Biskra**, for their continuous support and encouragement. To my dear family, I express my heartfelt thanks and gratitude for their love, moral support, financial assistance, and their endurance of the challenges of this academic journey.*

Contents

CHAPTER III :Thin films: Deposition and Analysis of results.

Figure list

Table list

GENERAL INTRODUCTION

Transparent oxide transporters are among the fascinating nanostructures that have significantly developed in recent years. These materials possess unique characteristics, and their nanoscale dimensions grant them exceptional ability to transport electrical charge with high efficiency and speed. Additionally, the high transparency of these oxides endows them with wide application potential across multiple fields.

Understanding these nanostructured oxides' physicochemical characteristics and behavior is crucial for developing new applications and enhancing existing techniques in areas such as transparent electronics, sensors, and energy storage. Therefore, we dedicated our work to the study of titanium oxide, which is highly regarded by researchers for its transparency, non-toxic nature, and ease of modification. We have chosen lithium for several reasons, primarily for its role in modification. We employed the sol-Gel method to compare our results with those of last year, specifically focusing on modifying titanium oxide with cesium.

Our work is structured into three chapters, each addressing specific aspects:

Chapter one serves as a review of transparent oxide transporters, including their properties, applications, and a detailed examination of titanium oxide, the main focus of our study. We provide an in-depth analysis of its optical, transport, and structural characteristics and general applications. Additionally, we discuss the modification process, highlighting lithium as the substance of interest in our research.

In Chapter two, we delve into thin films and their diverse characteristics and applications in research. We discuss the deposition methods for thin films and the techniques used for their characterization to extract the necessary information and interpret the obtained data effectively.

Finally, Chapter three presents a comprehensive examination of the experimental methodology, the tools utilized, and the anticipated results. We detail the experimental setup, including the instruments employed, and outline the expected outcomes of the study.

CHAPTER I

Titanium Dioxide: Properties and Applications.

Transparent conducting oxides (TCOs) are vital materials in modern technological applications due to their high electrical conductivity and optical transparency. These oxides include titanium dioxide (TiO_2), which will be the focus of this chapter. We will study the structural, electrical, and optical properties of TiO_2, as well as its various applications and the effect of lithium doping on its properties.

I.1. Transparent Conducting Oxides (TCOs)

Transparent conducting oxides (TCOs) are materials with high electrical conductivity that are optically transparent. TCOs have a transmittance of 80% and above in the visible spectrum, are characterized by an ultra-band gap (around 3eV) and have an electrical resistivity of more than $10^3(\Omega\ cm)^{-1}$. Since then, other TCO materials have been discovered, such as ZnO, In_2O_3, TeO_2, CuO, SnO_2, and TiO_2**[1]**.

I.1.1. Application of Transparent Conducting Oxides (TCOs)

Transparent Conducting Oxides (TCOs) are widely used in numerous new devices including solar cells, flat panel displays, gamma sensors, and many optoelectronic applications (**see figure I.1**). Nowadays, the high demand for flexible optoelectronic devices requires the development of efficient and non-costly TCOs deposited on substrates. Over the past decades, several new materials and manufacturing techniques have been developed to satisfy the technological requirements **[1]**

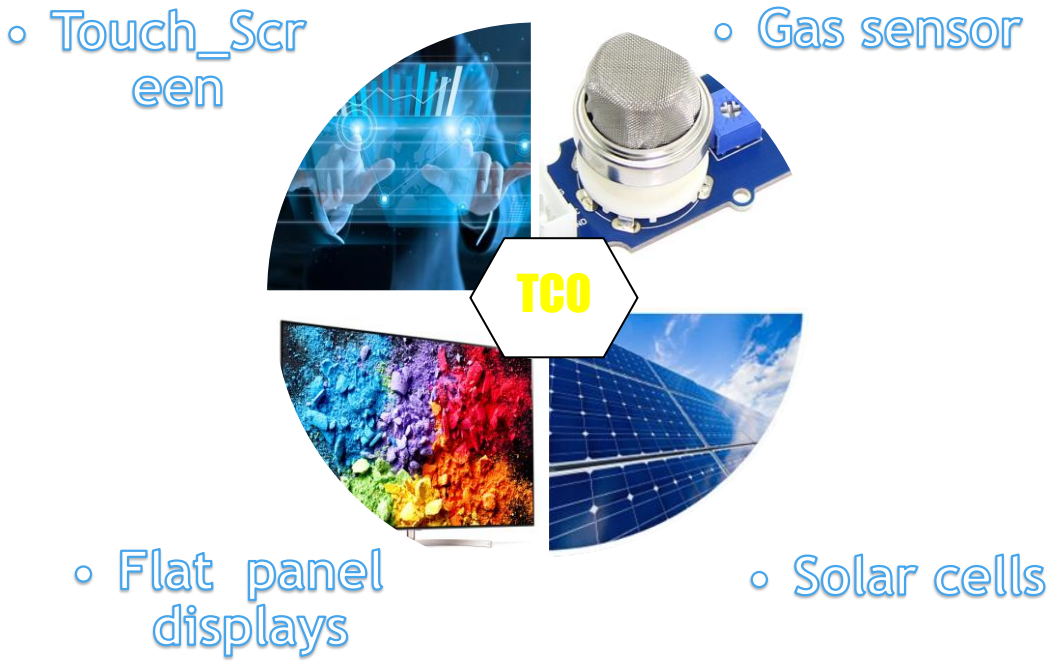

Figure I.1. Scheme of some Applications of Transparent Conducting Oxides.

I.1.2. Type of Transparent Conducting Oxides (TCOs)

Extrinsic semiconductors are classified as either n-type or p-type depending on whether the majority charge carrier is negative or positive.

- **P-Type oxides**

Transparent p-type conducting oxides mean that the majority of charge carriers are holes. This type is considered less common and limited compared to the n-type. One of the most important characteristics of transparent films was only 40% transparency, with a resistance of $1.4 \times 10^{-1}(\Omega.cm)$. After a few years, p-type oxide materials with better properties were discovered, such as NiO, CuO, PdO, La_2O_3, TeO_3, Ag_2O, and $BaTiO_3$ **[2-1]**.

- **n-Type oxides**

In this type of transparent conducting oxides, electrons are the majority of charge carriers. Therefore, they are the most common and widely used in practical applications **[1]**. **For examples**: TiO_2, SnO_2, TaO_5, In_2O_3, ZnO, and WO_3 [2].

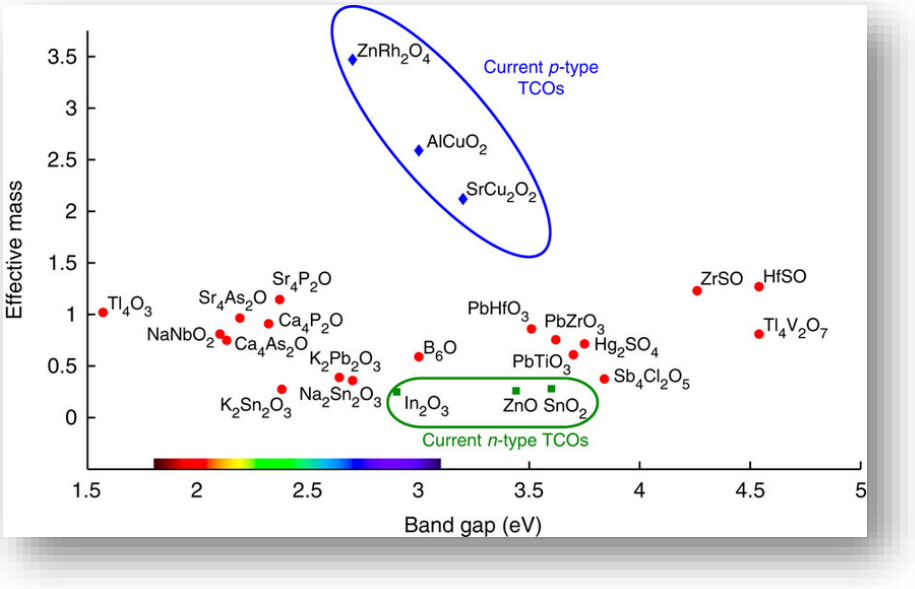

Figure I.2. Effective mass versus band-gap for the n and p-type TCO **[3]**.

I.2. Titanium Dioxide

Titanium is a metal that has high strength and low density. This makes it strong and light at the same time. However, it is not found in its pure form in nature because it has a strong attraction towards oxygen, carbon, and nitrogen. This makes it difficult to obtain in its pure state **[4]**. When exposed to air, titanium reacts with oxygen to form titanium oxide. It has several useful properties such as a high refractive index, high transparency as films, ultra band gap, and optoelectronic applications (active layers

in DSSC, AR coating for silicon solar cells…….). Furthermore, it is non-toxic, has chemical stability, high photosensitive tosunlight, for photocatalytic applications (water treatment, self-cleaning….)**[5]**.

Titanium dioxide occurs in three crystalline polymorphs: rutile, anatase, and brookite.

- Anatase: is more stable at low temperatures.
- Rutile: is thermodynamically the most stable phase and has the lowest surface energy.
- Brookite: is difficult to produce and is therefore not of practical interest.

The metastable anatase and brookite phases convert irreversibly to the rutile phase on heating above 700°C **[4]**.

I.2.1. Properties of Titanium dioxide

I.2.1.1. Structural properties

- **Anatase structure**

Anatase in a tetragonal crystal system exhibits a more complex structure than rutile. At high temperatures, typically around 700°C, anatase transforms into rutile. It contains titanium and oxygen atoms arranged in a specific way, with a characteristic bond length of 1.917 Å **[6]**. Is also an insulator with a band gap of about 3.2 eV whose lattice parameters are a = b = 3.784 Å and c = 9.515 Å **[5]** Anatase generally forms at lower temperatures than rutile or brookite and undergoes recrystallization at around 400°C It. Interestingly, it shares some properties with rutile, such as hardness and density **[6]**.

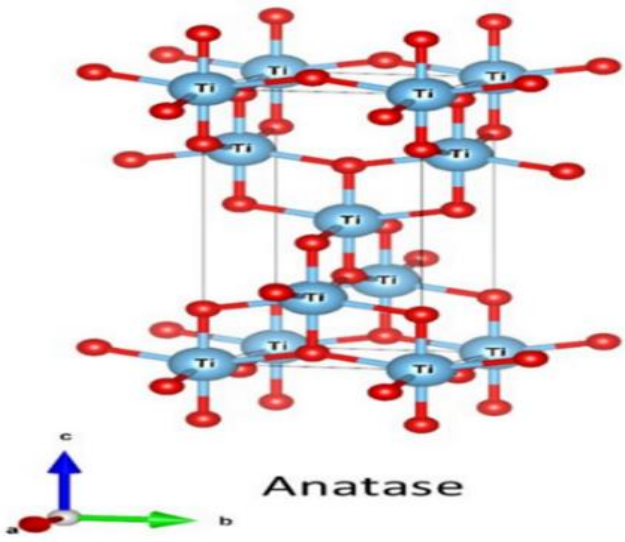

Figure I. 3. Anatase phase structure of TiO_2**[7]**

- **Rutile Structure**

Rutile has a very organized atomic structure. It belongs to a crystal system called tetragonal, whose lattice parameters are (a = b = 4.5936 Å, c = 2.9587 Å) **[5]**. where six oxygen (O) atoms surround each

titanium (Ti) atom. Interestingly, three neighboring titanium atoms form a nearly perfect triangle around a central titanium atom, all lying on the same flat plane. The average distance between a titanium and an oxygen atom (Ti-O bond) is about 1.959 Å. In comparison, the distance between neighboring titanium atoms (Ti-Ti bond) is slightly larger at 2.960 Å. It's important to note that rutile forms only under high-temperature conditions **[6]**.

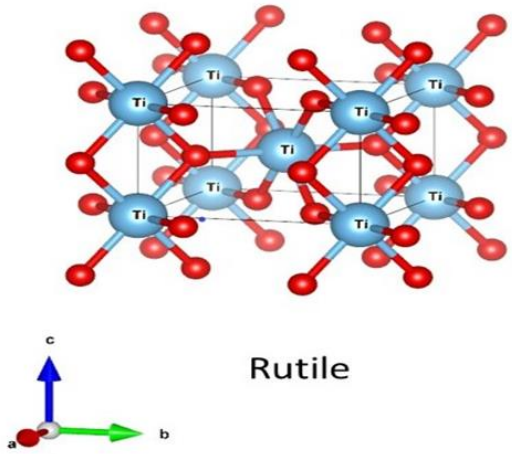

Figure I. 4. Rutile phase structure of TiO_2 **[7]**.

- **Brookite Structure**

Brookite crystallizes in an orthorhombic system, with a complex structure similar to other structures. Pure brookite synthesis is difficult, and the brookite phases turn into rutile at high temperatures (750 °C) **[6]**. Its mesh parameters are a = 9.184 Å; b = 5.447 Å; c = 5.145 Å **[5]**.

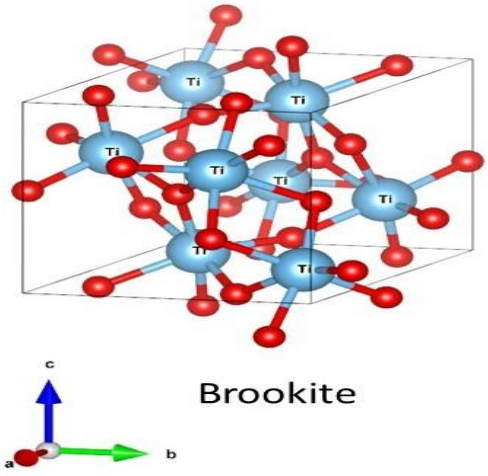

Figure I. 5 Brookite phase structure of TiO_2**[7]**.

I.2.1.2 Optical properties

- **Transmission spectrum**

TiO_2 exhibits a high transparency (> 60 - 95%) in the visible (depending on thickness), in the UV region, UV light absorption predominates for short wavelengths (< 380 nm). This gives it important qualities like protection from UV radiation **[8]**.

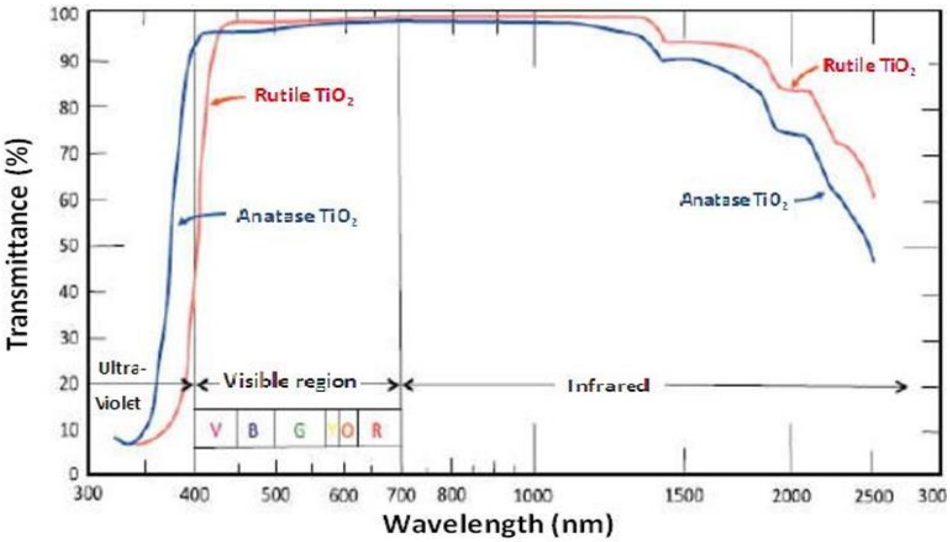

Figure.I.6 Transmittance of TiO_2**[9]**.

- **Optical gap**

As a result, TiO_2 is described as a semiconductor material with a large bandgap. The values of the Rutile, Anatase, and Brookite gaps, respectively, are 3 eV, 3.2 eV, and 3.1 eV **[6-10]**.

- **Refractive index**

In the visible spectrum, the various forms of titanium dioxide have a high refractive index n. Out of the three stable crystal phases, the Rutile variety has the highest index (n~2,66) compared to the Anatase variety's (n ~ 2,54)**[6]**. and the brookite (2,586) **[11]**. When combined with an elevated visible light dispersion coefficient, Rutile becomes the preferred white pigment for the food, pharmaceutical, and painting industries **[10]**.

I.2.1.3. Electronic properties

Titanium Dioxide is an n-type semiconductor, the TiO_2 single crystals have a resistivity of about $10^{13}\Omega$.cm at room temperature, and about $10^{7}\Omega$.cm at 250 °C. TiO_2 is generally considered an insulator at temperatures below 200 °C, However, the electrical properties of the TiO_2 film can be modified to become highly conductive for many applications such as humidity and gas sensors **[6-8]**.

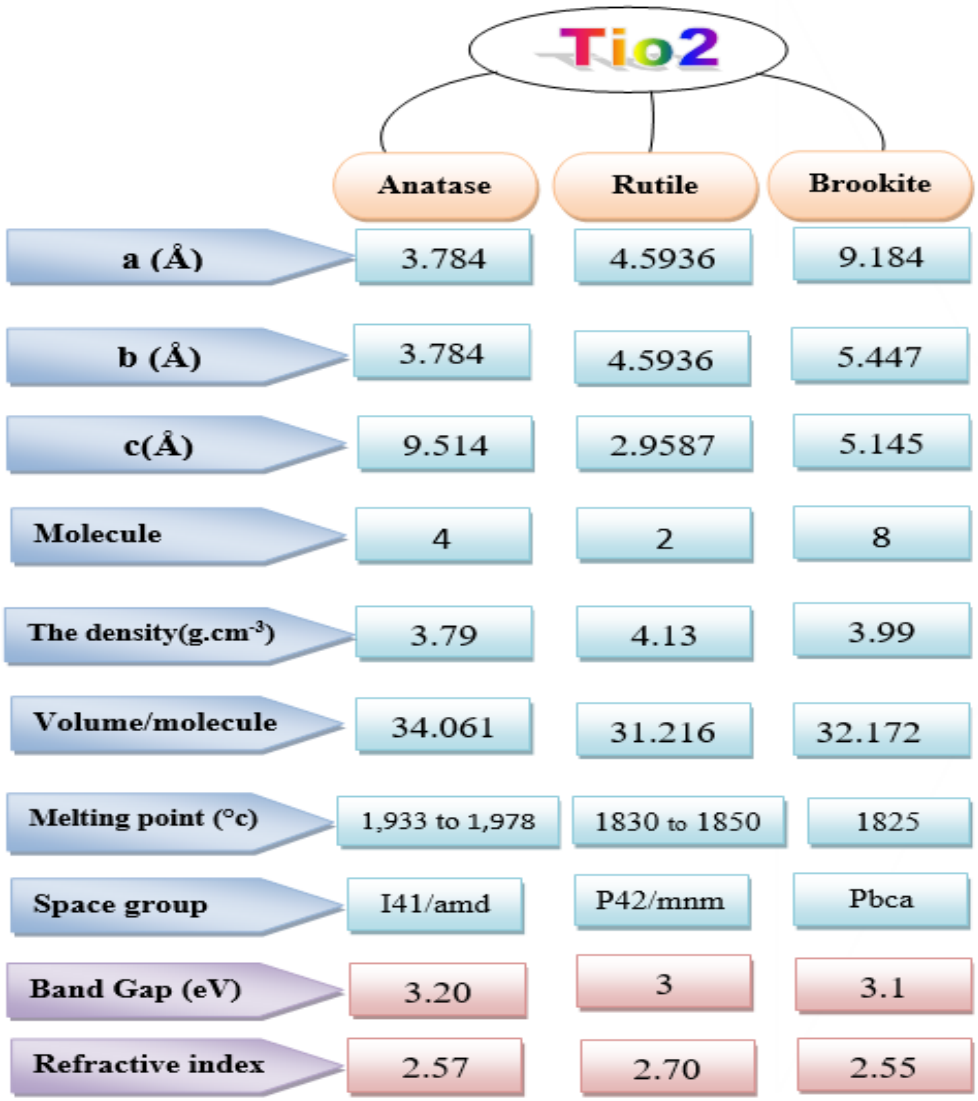

Figure I. 7. Flowchart of the Structural and Optical properties **[12-8-6].**

I.2.2. Applications of titanium dioxide

titanium dioxide has excellent semiconductor properties, which has generated significant enthusiasm on the part of scientists for various applications, and in particular for photocatalysis, photovoltaic cells, biocompatible products, antireflection coatings, optical waveguides, devices based on metal, insulator, ferroelectric, electrochemical biosensors, and antibacterial application **[13]**.

Figure I. 8. Flowchart of the titanium dioxide applications**[14]**.

I.3. Doping

The doping process is critical in semiconductors, as it helps improve the material's properties according to the desired application field. Among these properties are optical, electrical, electromagnetic, and structural properties. The doping of TiO_2 oxide with transition metals is one of the most important approaches and several doping works have been carried out with different metals: Iron, Zirconium, Cerium, Manganese, Chromium, Cobalt, Tungsten, and Lithium.

Doping sites are not limited to replacing atoms Ti^{4+} or O^{2-} ions in the structure with metal or non-metallic substitutes. But, it can also be located in interstitial positions between Ti^{4+} and O^{2-} sites. Doping species are generally incorporated into the structure to reduce the energy value of the band gap (by lowering the conductive band's upper edge or raising the valence band's lower edges). This has the effect of sensitizing TiO_2 to visible range wavelengths **[15]**.

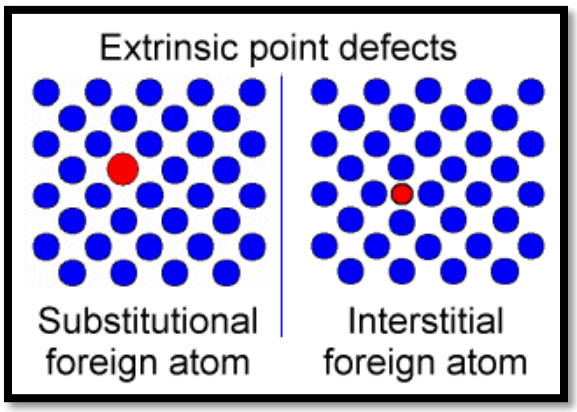

Figure I. 9. Schematic of defining of defects **[16]**.

The state of affairs is as follows:

- **n-type doping:**

In this category of transparent conductive oxides, electrons are the primary charge carriers, with the majority being of the n-type variety. These n-type oxides are prevalent in practical applications due to their widespread use and effectiveness **[17]**.

- **p-type doping**

Transparent p-type solids are relatively scarce and restricted compared to their n-type counterparts, prompting increased research efforts to acquire this type. A crucial characteristic o
p-type materials are holes that serve as the predominant charge carriers, imparting a p-type character to the material **[17]**.

I.3.1. Lithium

Lithium is a metal with the lowest atomic weight and highest negative potential**[18]**. There is a long history of using lithium compounds in conventional industrial applications. There are more recent uses in the fields of health, chemistry, and energy storage (batteries) **[19]**.

Lithium is an alkali metal with an atomic number = 3, and an atomic mass of 6.941 g/mol. Lithium has 3 protons, 3 electrons, and 4 neutrons. Being an alkali metal, which is soft and flammable. It also has a low density and under standard conditions, it is the least dense solid element. It is less dense than water (with which it reacts) and forms a black oxide in contact with air **[20]**.

Table I.1. Properties of lithium**[20]**.

Single quotation mark	**Atomic Number**	**Atomic Mass**	**Density**	**Color**
Li^{3+}	3	6.941 g/mol	0.534 g/cm^3	Light silver
Melting point	**Crystal structure**	**Magnetism**	**Electronegativity**	**Oxidation states**
453.69 k	Body-centered cubic	paramagnetic	0.98	+1,−1

CHAPER II

Titanium Dioxide: Deposition and characterization techniques.

In this chapter, we will review various doping techniques and their effects on target materials. We will also discuss thin film deposition methods, including physical vapor deposition (PVD) and chemical vapor deposition (CVD), and their importance in applications such as electronics and solar energy. Finally, we will address characterization techniques like UV-visible spectroscopy and X-ray diffraction, which enable the precise analysis and evaluation of thin film properties, contributing to the improvement of product quality and the development of new materials in the industry.

II.1. Thin films

II.1.1. Thin Films and its Properties

A thin film is a Nanostructure or layers of material atoms with a thickness typically less than 1 µm or several nanometers, arranged in a two-dimensional configuration, where the third dimension is significantly smaller than the nanoscale. In solid-state physics, the influence of surfaces on material properties is often disregarded. However, in the context of thin layers, surfaces play a significant role and can greatly impact material properties **[17]**.

II.1.2. Thin film growth mechanisms and modes

The microscopic structure of the thin layers is susceptible to the physical and chemical properties of the material, as well as the physical conditions for deposition at every stage of the development of the thin layer so all the methods are subject to the following stages: atoms, serum, and growth.

There are three patterns of thin layer growth **[21]**:

- three-dimensional(3D) growth pattern (Weber Volume).
- two-dimensional(2D) growth pattern (Frank-Van der Merwe).
- mixed pattern (Krastanov-Stranski).

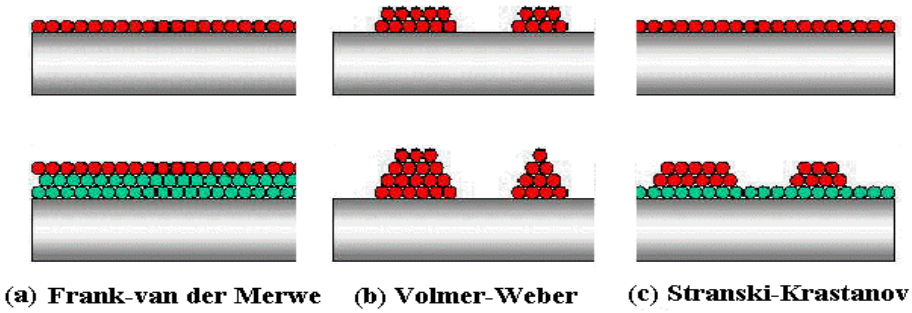

Figure II. 1. Different thin films growth mechanisms **[22]**.

II.1.3. Thin films applications

In the recent years TiO_2 films are extensively studied because of their interesting chemical, optical and electrical properties. TiO_2 thin films have received great attention, because of having excellent properties **[23]**.

Numerous applications exist for titanium dioxide, which can be categorized into four groups based on its optical, photocatalytic, electrical, and hydrophobic properties **[11]**.

We can mention a few applications like:

II.1.3.1 Photocatalytic applications

Heterogeneous photocatalysis is an advanced oxidation process that uses oxidizing catalysts to break down organic compounds into water and CO_2 by generating hydroxyl radicals (OH). This technique involves exposing a semiconductor like titanium dioxide (TiO_2) to UV radiation, either from sunlight or a UV lamp. Electrochemically, the process relies on electronic reactions at the catalyst's surface (TiO_2). It can be summarized into four steps**[24]**:

a) Production of electron/hole pairs: UV photons excite TiO_2, causing electrons to move from the valence band to the conduction band, creating oxidation (holes h+) and reduction (electrons e^-) sites.

b) The second step involves separating electrons and holes to prevent recombination, which is achieved by trapping free charges using structural irregularities or adsorbed molecules.

c) Charges on the catalyst react with adsorbed substances, leading to oxidation (electrons with oxygen) and reduction (holes with electron donors), crucial for pollution control.

d) Oxidative radicals break down pollutants into water and CO_2, but recombination limits efficiency. Research explores doping and adding electron acceptors to enhance hydroxyl radicals (OH°).

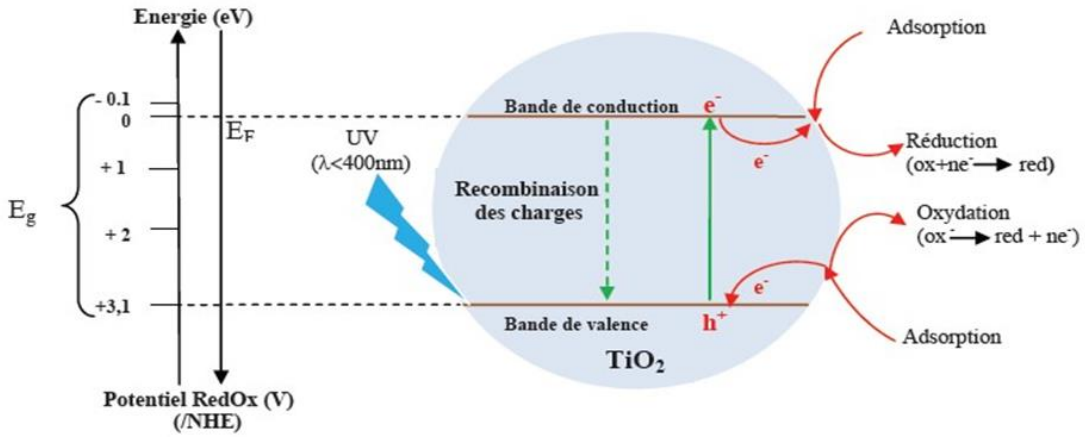

Figure II.2. Diagram of the photocatalytic process in an anatase TiO_2 thin films **[24]**.

II.1.3.2 UV protection

Ultraviolet (UV) rays, with wavelengths ranging from 200 to 400 nm, are known for their harmful effects on skin health. They are categorized into UVC (200-290 nm), UVB (290-320 nm), and UVA (320-400 nm). While UVC is blocked by the atmosphere, UVB causes sunburn and can be blocked by glass. However, UVA can penetrate glass and cause skin damage, including skin cancer. Sunscreen, either organic or inorganic, is commonly used for protection. Inorganic sunblocks like TiO_2 effectively protect against UVA and UVB due to their semiconductor properties. TiO_2 absorbs UV rays by generating and separating photo-generated electrons and holes. Its high refractive index also contributes to UV reflection and scattering, enhancing its UV-shielding properties. Besides skin protection, TiO_2's UV-blocking abilities benefit the textile industry by reducing photochemical degradation and color fading of fibers exposed to UV radiation **[25]**.

II.1.3.3 The photochemistry

In the field of photochemistry, titanium dioxide allows the initiation of reactions such as photolyase of water, photo-reduction of nitrogen, and purification of effluent liquids and gaseous. These phenomena are based on the creation of pairs electron-trou when the photons used have energy superior to the banned band TiO_2, thus generating an oxide-reduction system **[26]**.

II.1.3.4 solar cells

Solar energy is a clean, abundant, and renewable energy. The current technology for converting sunlight to electrical power is silicon-based solid-state solar cells. In recent years, new semiconducting material-based solar cells have emerged to offer possible alternative photovoltaic technology with the prospect of cheap fabrication and flexibility**[27-2]**. Nano-structured TiO_2 has been the main semiconducting material for this new generation of solar cells. In this technology, an electron sensitizer absorbing in the visible is used to inject charge carriers across the semiconductor-electrolyte junction into TiO_2 to enhance the conversion efficiency from solar energy, because TiO_2 with its band gap of 3.2 electronvolt (eV) absorbs only the ultraviolet part of the solar energy. This type of solar cell is therefore called a dye-sensitized solar cells (DSSCs) **[28]**.

II.1.4. Thin Films Deposition Process

The thin slice technique has become the focus of most researchers on the impressive results obtained in several areas, the most important of which are vector and access devices. The thin membrane technique is based on 3 bases of manufacture, description, and application **[29]**. These deposition methods have been diversified and classified into two main parts, deposition of physical vapor (PVD) and deposition of chemical vapor (CVD) as (**shown in figure II.3**):

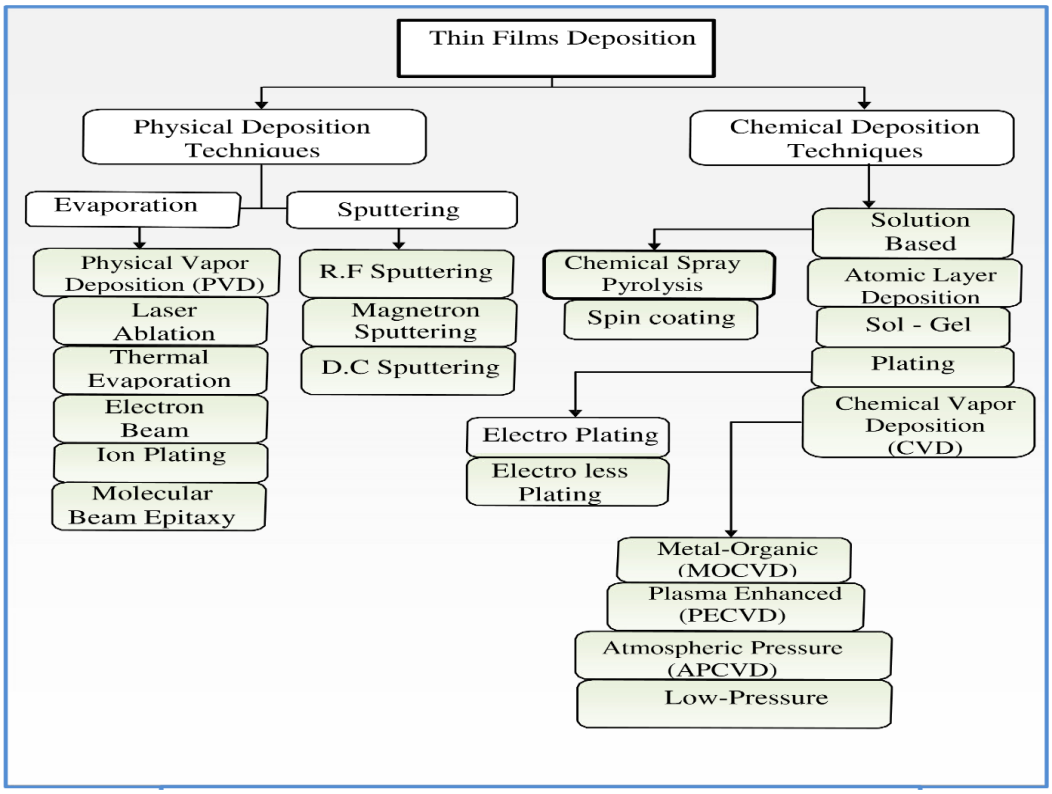

Figure II. 3. Classification of thin film deposition techniques **[30]**.

II.1.4.1. Physical deposition Method (PVD)

- **Pulsed Laser Deposition (PLD)**

Pulsed laser deposition (PLD) represents a sophisticated evaporation technique employed in thin film fabrication. Within a controlled vacuum environment, high-energy laser pulses are utilized to vaporize the target material. This action generates a plasma plume, subsequently deposited as a thin film onto a substrate. The PLD process encompasses distinct phases including evaporation, ablation, plasma formation, and exfoliation, rendering it intricate compared to alternative methods. Despite its complexity, PLD offers notable advantages such as elevated deposition rates**[31].**

- **Sputtering**

Sputter deposition is a method for sputtering PVD into thin-film deposition. This includes expelling deposited material on the “top” just in case of a source to a “substrate” which usually happens in a silicon wafer. Reemission by ion or atom bombardment of the deposited material during the deposition process is done by reuttering.

Atoms that are expelled by sputtering from the target have an energy distribution range that is very wide, typically as much as equal to multiples of tens of eV. The presence of various criteria controlling sputter deposition makes it a difficult process but also allows experts to track the film’s growth and microstructure to a large extent **[32]**.

II.1.4.2. Chemical Deposition Method (CVD)

Chemical methods utilized for the fabrication of thin films encompass liquid phase methodologies such as spray pyrolysis, sol-gel, spin-coating, and dip-coating, as well as gas phase approaches like chemical vapor deposition (CVD) and atomic layer epitaxy (ALE). CVD, for instance, relies on volatile chemicals to decompose on a heated substrate to generate a non-volatile film constituent and a pumpable vapor or gas. This technique finds applications in a variety of fields including the production of automotive components, and medical devices. Conversely, the liquid phase techniques offer a more straightforward and cost-effective means for molecular material design. Furthermore, the implementation of chemical processes like pyrolysis, reduction, oxidation, and compound synthesis in CVD facilitates the creation of high-performance thin films **[33]**.

- **Spray pyrolysis**

The spray pyrolysis deposition technique is a method commonly employed in materials science and the fabrication of thin films. Using an atomizer, a mixture of several reactive chemicals is vaporized and then projected onto a heated substrate so that the base temperature is important to stimulate chemical reactions between compounds.

Through thermal decomposition, the precursor material transforms into the desired thin film. Spray pyrolysis is known for its simplicity, cost-effectiveness, and versatility, making it a popular choice for various applications in electronics, optics, and renewable energy **[34-30]**.

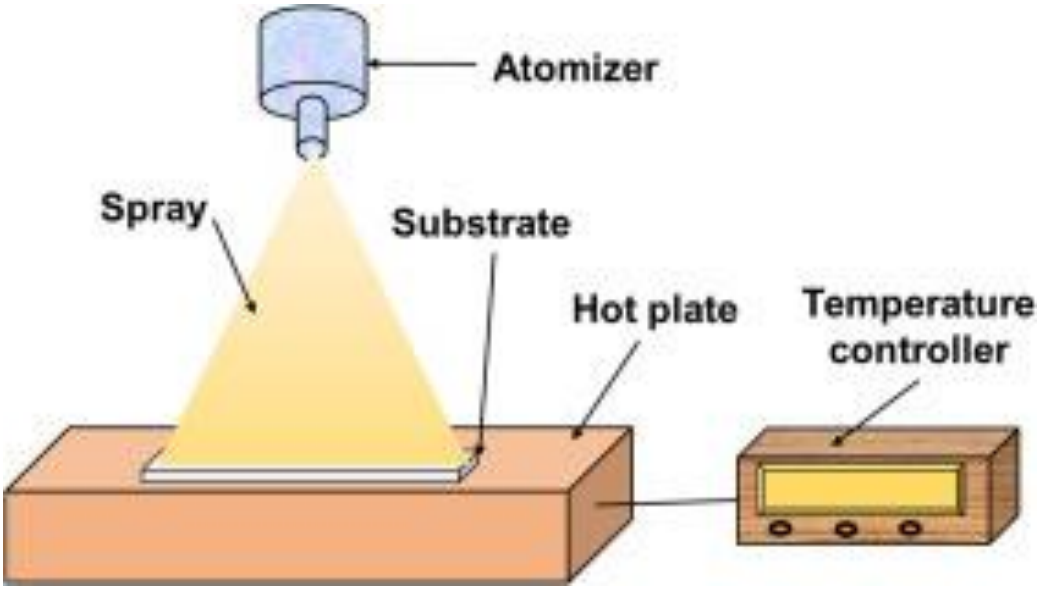

Figure II.4. Schematic of Spray pyrolysis process **[35]**.

- **Sol-gel**

The world has known jelly solution technology for over 150 years**[22]**.The term Sol-Gel refers to the abbreviation "Solution-Gelation." Briefly, a "Sol" is a colloidal suspension of oligomers whose diameters

are only a few nanometers. Subsequently, this "sol" can evolve through chemical reactions into a lattice with infinite viscosity, called a "Gel"**[36]**.

In this work, the choice of methods for the elaboration of thin layers of TiO_2 was made based on the sol-gel method due to its numerous advantages.

II.2. Sol-Gel Method

II.2.1. The principle of Sol-Gel

The sol-gel method is highly interesting for producing ceramic materials, powders, fibers, and thin films. The basic idea of the sol-gel process is simple: a mixture of liquid precursors transforms into a solid through a series of relatively low-temperature chemical reactions. Two types of methods can be employed, leading either to colloidal gels or polymeric gels (**Figure II.5**). The precursors used are either inorganic salts (chlorides, nitrates, etc.) or molecular compounds (Alkoxides, acetates, etc.). They are dissolved in a suitable solvent. The resulting solution is hydrolyzed. This results in either a colloidal suspension of fine particles or the formation of a polymer-type network. Hydrolysis leads to a gel which, after drying, results in a solid (Xerogel). This can be further transformed into a powdery material, fiber, film, or glass through appropriate thermal treatment **[26]**.

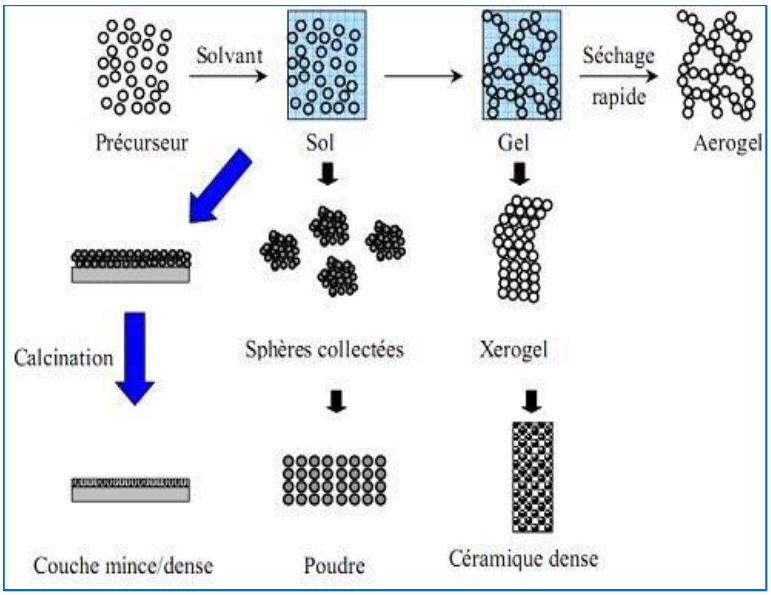

Figure II.5. Diversity of sol-gel materials and their forming **[8]**.

II.2.2. Sol-Gel process

There are two synthesis routes for the Sol-gel process**[26]**:

II.2.2.1. Solution based on an Inorganic (or colloidal) precursor

This is conducted using metal salts (chlorides, nitrates, oxychlorides) in aqueous solution. This route is inexpensive but difficult to control, which is why it is still not widely used. However, it is the preferred route for obtaining ceramic materials.

II.2.2.2. Solution based on an organic (or polymeric) precursor

This route involves using metal Alkoxides in organic solution to obtain gels. It is relatively expensive but allows for fairly easy control of particle size. The most commonly used precursors in the Sol-gel process are metal Alkoxides with the general formula $M(OR)_n$, where M represents a metal of valence n and R represents an alkyl chain of the type ($-C_nH_{2n+1}$).

The precursors can be of very high purity and have high solubility in a wide variety of organic solvents. In both cases, the reaction is initiated by hydrolysis, leading to the formation of M-OH groups, followed by condensation, allowing the formation of M-O-M bonds.

II.2.3. Chemical reactions in the Sol-Gel

The Sol-Gel process relies on two reactions**[26]**:

- Hydrolysis, which corresponds to the activation reaction.
- Condensation-polymerization, which is the chain growth step.

II.2.3.1. Hydrolysis

This involves a reaction between a water molecule and an alkoxide, resulting in the formation of an alcohol molecule:

$$M(OR)_4 + H_2O \rightarrow HO - M(OR)_3 + ROH \quad \text{(II. 1)}$$

This reaction is initiated either by adding water or a water/alcohol mixture to a metal alkoxide, or by changing the pH of the solution **[26]**.

II.2.3.2. The Condensation

The -OH groups generated during hydrolysis are good nucleophiles and, during condensation, lead to the formation of M-O-M bridges during condensation, two competitive mechanisms must be considered **[36-26]**:

- **The Alkoxalation**

  Alkoxalation refers to a chemical reaction wherein an alcohol molecule is eliminated during condensation, leading to the creation of "oxo" bridges that connect two metal atoms via the bond denoted as (M-O-M):

  $$(OR)_{n-1} - M\text{-}OH + RO\text{-}M\text{-}(OR)_{n-1} \rightarrow (OR)_{n-1}\text{–}M\text{-}O\text{-}M\text{–}(OR)_{n-1} + R\text{-}OH \quad \text{(II. 2)}$$

- **The oxidation**

This process takes place between two partially hydrolyzed alcoholates. The mechanism remains unchanged, except that the leaving group is now a water molecule.

$$(OR)_{n-1} – M\text{-}OH + HO\text{-}M\text{-}(OR)_{n-1} \rightarrow (OR)_{n-1}–M\text{-}O\text{-}M–(OR)_{n-1} + H_2O \quad (II.\ 3)$$

When these two reactions are completed, a gel is obtained. The transformation of the solution into a solid polymeric mass is generally referred to as the sol-gel transition.

II.2.4. Sol-Gel Transition

As the hydrolysis and condensation reactions progress, polymeric clusters, whose size increases with time, are formed. When one of these clusters reaches an infinite dimension (practically the size of the container), the viscosity also becomes infinite: this is the point of the Sol-Gel transition. From this moment on, the infinite cluster (gel fraction) continues to grow by incorporating the smallest polymeric groups. When all the bonds have been utilized, the gel is formed. From a macroscopic perspective, the transition can be tracked by the mechanical behavior of the solution. It is characterized by the divergence of the solution viscosity and an increase in the elastic constant in the gel phase G (or Coulomb modulus) The evolution of the viscosity of a sol and its Coulomb modulus, are schematically presented in (**Figure II. 6**), as a function of time: at the complete formation of the gel, the viscosity becomes infinite, while the elastic constant tends toward its maximum value. The solid mass formed contains trapped liquid masses. Their removal occurs through evaporation**[5]**.

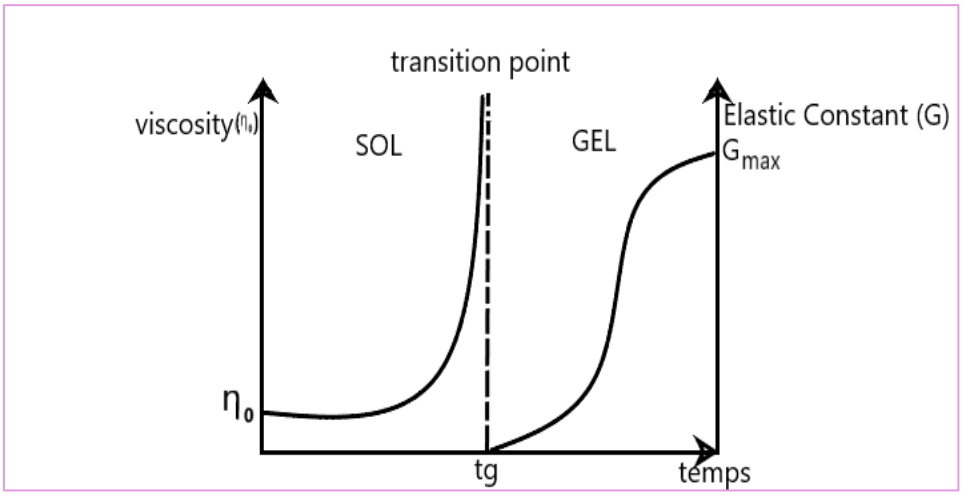

Figure II.6. Evolution of the sol viscosity and the elastic constant of the gel, tg being the time corresponding to the Sol-Gel transition**[5]**.

II.2.5. Heat treatment

II.2.5.1. Drying

One of the images is printed, the material undergoes drying due to capillary forces in the pores, and this drying results in a volume recovery that allows for the installation of the Sol-Gel mat necessary to remove alcohol or water when the gel is solid. The vaporization process is made of a beautiful and hard product found in the Sol-Gel pores.

Several types of designs allow different types of material**[37]**:

- **Aerogel**

This classic drying (normal evaporation) results in a volume reduction of 5 to 10%. The evaporation of the solvent allows the formation of a Xerogel which can be subjected to heat treatment at moderate temperature to densify the material. Densification temperatures strongly depend on the type of material and the desired properties. Drying the gel is a delicate step. The solvent must evaporate very slowly to avoid fragmentation of the Xerogel. Producing a solid material is therefore difficult due to the internal tensions appearing during drying which can lead to the cracking of the material

- **Xerogel**

This is drying under critical conditions (in an autoclave under high pressure) resulting in little or no volume shrinkage. The evacuation of the solvent under supercritical conditions leads to the formation of an air gelthat has not undergone any densification. We thus obtain a very porous material with exceptional properties. The transition from "sol" to "gel", whose viscosity can be controlled, also allows the production of fibers and films on various supports by dipping or vaporization.

II.2.5.2. Annealing

Heat treatment or annealing allows on the one hand the elimination of residual organic species after drying, and on the other hand the densification of the material by crystallization. It is only after annealing that the desired material can be obtained. Indeed, after drying, organic groups of the alkyl type (-OR) are still present in the deposited film. Only annealing can eliminate them. Annealing is generally carried out at temperatures between 300 °C and 1400 °C depending on the type of substrate**[8]**.

II.2.6. Deposition of Thin Films by Sol-Gel

Several techniques can be used for depositing thin layers on a given substrate via the sol-gel route: spin-coating, drain-coating, and dip-coating, each with its characteristics.

The choice of deposition method depends on the characteristics of the substrates such as their geometry or size, as well as the geometric properties desired for the thin layer. The two methods presented below are the most commonly used **[26]**.

II.2.6.1. Dip-coating process

In the dip coating process, film formation takes place by evaporation of the solvent from a polymer solution. The substrate is dipped into the polymer solution, taken out at a constant speed, and dried by allowing the solvent to evaporate, leaving behind a solid polymer film on the substrate. Griffin et al **[38]** divided the dip coating process into five stages: (a) immersion, (b) start-up, (c) deposition, (d) drainage, and (e) evaporation, (**shown in Figure II.7**).

The thickness of the coating layer depends on the following factors**[39]**:

- The speed of substrate withdrawal.
- Solution concentration.
- Solution viscosity.
- Solvent evaporation rate.
- Substrate withdrawal angle.

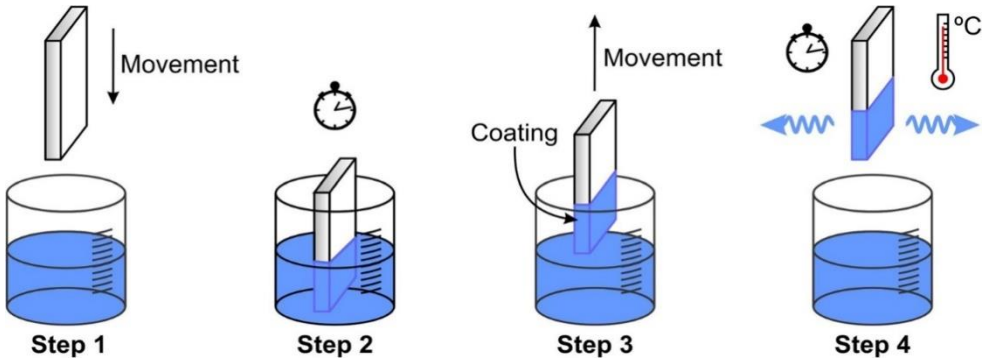

Figure II. 7. Schematic of Dip-Coating process **[40]**.

II.2.6.2. Spin coatingprocess

II.2.6.2.1. An Overview ofSpin-Coating

Spin coating is a widely used method for creating consistent and even thin films ranging from nanometers to microns in thickness on substrates **[27]**. leveraging centripetal force and surface tension. Initially, a small volume of the coating solution is deposited at the center of the substrate using a micropipette. Subsequently, the substrate undergoes rapid spinning for a brief duration (usually a few seconds) to uniformly spread the coating material across its surface, where the substrate rotates while the precursor solution is applied. A vacuum is essential to secure the substrate onto the spinning holder throughout the coating process. Each layer of the coating is dried by solvent evaporation before the subsequent coating cycle. This sequence repeats until achieving the desired thickness of the coating layer. The resulting film thickness is contingent upon various factors including spinning speed, solution viscosity, concentration, and solvent type. Spin coating offers the advantage of efficiently producing uniform thin films of diverse thicknesses with ease and speed **[41]**.

These steps of thin film deposition are schematically illustrated in **Figure II.17**:

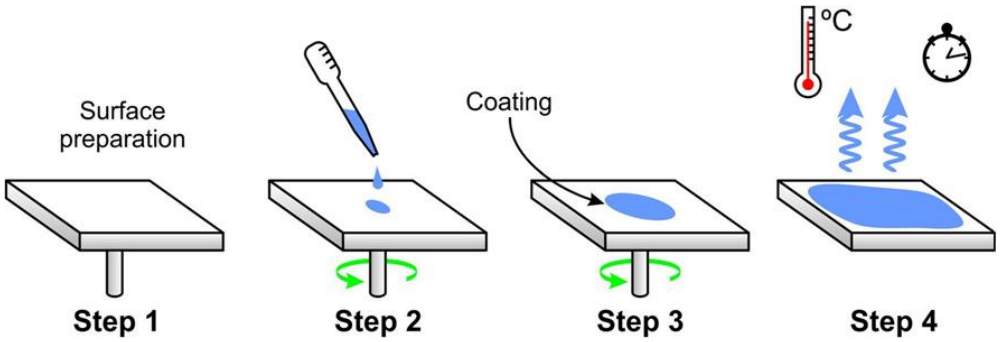

Figure II. 8. schematically illustrates the thin film formation process via spin coating **[40]**.

II.2.6.2.2. Spin Coating Applications

Spin coating finds extensive application across a diverse range of industries and technologies. It can effectively coat substrates of various sizes, from small millimeter-scale substrates to large flat panel displays measuring meters in diameter. This technique is utilized for coating substrates with a plethora of materials, including photoresists, insulators, organic semiconductors, synthetic metals, nanomaterials, metal and metal oxide precursors, transparent conductive oxides, and more. Furthermore, spin coating is more used in the fields of semiconductor and nanotechnology research and development, as well as industrial sectors, showing its versatility and indispensability **[27]**.

II.2.6.2.3. Advantages and disadvantages of Spin Coating

This method boasts numerous advantages, making it highly desirable Among these benefits are **[4]**:

- Doping facilitated in large quantities.
- Feasibility of multicomponent coatings by mixing the corresponding alkoxy in the starting solution.
- Ability to produce thin layers of inorganic oxides at low temperatures on heat-sensitive substrates.
- Doping facilitated in large quantities.

Some disadvantages **[39]** of the sol-gel process are:

- High cost of raw materials.
- Large shrinkage during processing that accompanies drying and sintering.
- Residual fine pores.
- Residual hydroxyl and carbon.
- Health hazards of organic solutions.
- Long processing times.

II.3. Characterization of thin film properties.

Following the deposition of thin films, the immediate step involves studying their physical and chemical properties. This stage is considered crucial for researchers, as it allows for the interpretation of

obtained results, whether desired or undesired. It also involves linking these results to the application and development of these properties. Various techniques are employed to determine the overall properties, which change according to their field. These include structural, morphological, optical, and electrical properties, among others **[2]**.

II.3.1. Adhesion test

Before conducting any characterization on the as-prepared and heat-treated films, we assessed the adhesion strength between the films and the substrates by conducting a Scotch tape test on the deposited films. Typically, adhesion strength is deemed "good" if the film remains adhered to the substrate without peelingoff **[42]**.

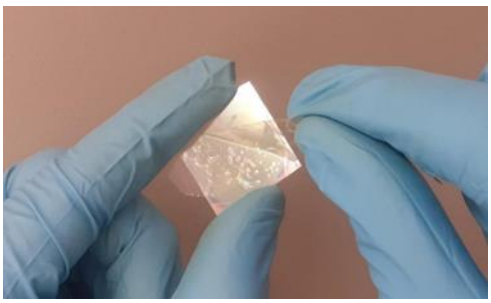

Figure II.9. Simple adhesive tape tests.

II.3.2. Structural characterization

II.3.2.1. X-Ray diffraction

X-ray diffraction studies were conducted to examine the crystallographic properties of the prepared thin film. Each substrate produces a characteristic X-ray diffraction pattern, indicating whether it is in a pure state or part of a mixture. This principle underlies the diffraction method of chemical analysis. Diffraction analysis is advantageous for determining the chemical combination and phase of elements, as it is faster, requires only a small sample, and is non-destructive compared to conventional methods **[4]**. The X-rays serve as the foundation for other analytical techniques, including radiography, spectroscopy, and diffractometry **[43]**.

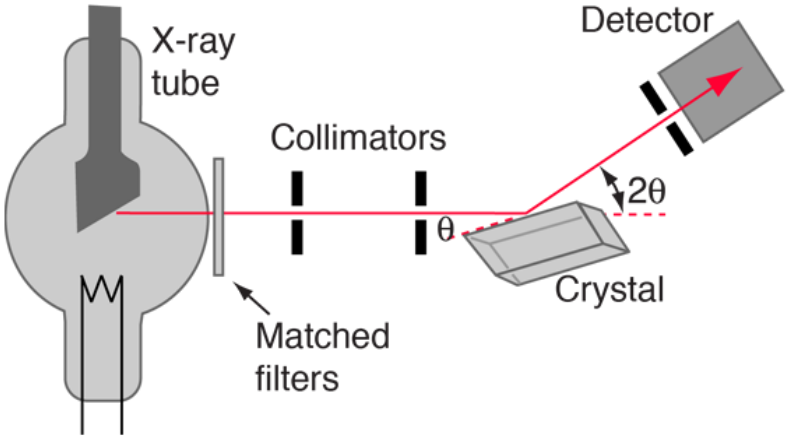

Figure II. 10. Principle of X-ray powder diffraction [44].

II.3.2.2. Bragg's Law

Bragg's law describes the diffraction of X-rays by crystals, stating that when X-rays are incident upon a crystal, they scatter from the atoms within the crystal lattice. These scattered X-rays then interfere with each other, with constructive interference occurring only when the path difference between them is an integer multiple of the X-ray wavelength. These electromagnetic radiations have an onde length of the Ångström order (1 é = 10^{-10}m) **[43-45]**.

The equation for Bragg's law is:

$$n\lambda = 2d_{hkl} \sin\theta \qquad \text{(II.4)}$$

where:

n: the diffraction order (1, 2, 3, ...).

λ : the wavelength of the X-rays.

d_{hkl}: the spacing between the atomic planes in the crystal.

Θ : the angle of incidence of the X-rays.

Bragg's law is used to determine the structure of crystals. By measuring the angles at which X-rays are diffracted by a crystal, scientists can calculate the spacing between the atomic planes in the crystal. This information can then be used to determine the crystal structure **[45]**.

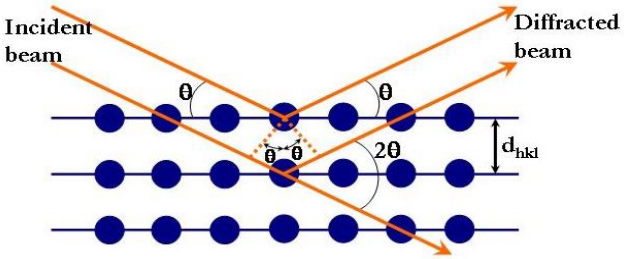

Figure.II.11. Schematic description of the diffraction of lattice planes according to W. L. Bragg [60].

II.3.2.3. Determination of the crystal size

The size of crystallites was calculated using the well-known Scherrer's formula **[46]**:

$$D = \frac{0.94\lambda}{\beta\cos(\theta)} \qquad \text{(II.5)}$$

Where:

D: the crystallite size.

λ: the wavelength of X-rays(λ =1.5405 Å).

β(**FWHM**): represents the broadening of the diffraction line measured at half maximum intensity in radians.

θ : The Bragg angle.

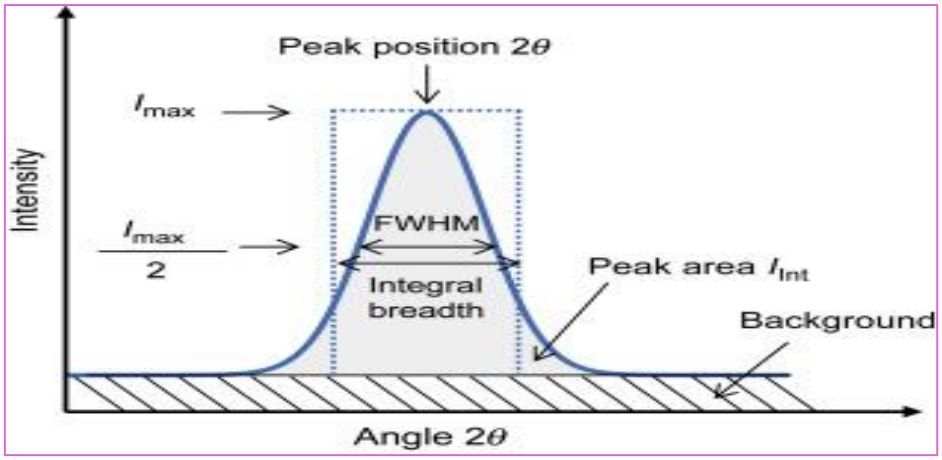

Figure II. 12. The width at half the height of the peak (FWHM) [47].

II.3.2.4. The dislocation density (δ)

The dislocation density given in (equation II.6) is defined as the length of dislocation lines per unit area in the film, and can be calculated using the crystallite size (D) **[12]**:

$$\delta = \frac{1}{D^2} \qquad \text{(II.6)}$$

II.3.2.5. Micro-Strain (ε)

We calculate strain from the following equation **[12]**:

$$\varepsilon = \frac{\beta}{4\tan(\theta)} \qquad \text{(II.7)}$$

II.3.3. Optical properties

II.3.3.1. UV-Visible Spectroscopy

UV-visible spectrophotometry is based on the interaction between electromagnetic radiation and matter in the spectral fields of UV-visible and near-infrared. This method allows us to measure the transmittance (or absorbance) as well as the reflectivity **[9]** (**Fig.II. 13**).

This technique is crucial for determining the color of chemicals as it measures how much light passes through a sample (I)compared to the initial light intensity (I_0). This ratio, known as transmittance, is typically expressed as a percentage (T %). Absorbance (A) is calculated from transmittance using the formula:

$$A = -\log(\frac{T}{100}\%) \quad (II.8)$$

In the spectral field where light is absorbed, the layer thickness and the absorption coefficient can be calculated for each permeability transfer value using the following phrase **[48]**.

$$\alpha = \frac{1}{d}\mathrm{Ln}(\frac{1-R}{T}) \quad (II.9)$$

The UV-visible spectrophotometer can be also configured to measure reflectance. In this case, the spectrophotometer measures the intensity of light reflected from a sample (I) and compares it to the intensity of light reflected from a reference material (I_0). The ratio (I / I_0) is called reflectance and is usually expressed as a percentage (R %) **[49]**.

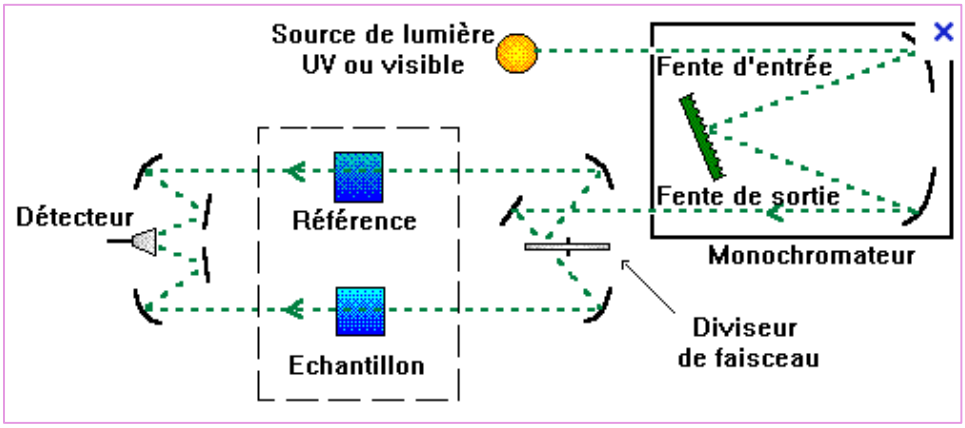

Figure II. 13. schematic representation of the spectrophotometer **[50]**.

II.3.3.2. The film thickness measurement

We used two methods to measure the thickness of our samples

- **Interference fringe method**

Using the physical parameters that are defined in the figure and the transmission spectra obtained, we can determine the thickness of the film as follows

$$d = \frac{\lambda_1\lambda_2}{2(\lambda_1 n_2 - \lambda_2 n_1)} \quad (II.10)$$

The refraction indices of the film for wavelengths λ_1 and λ_2 are denoted by n_1 and n_2, respectively. n_1 and n_2 can be computed using the following formula **[30]**:

$$n_{1,2} = [\, N_{1,2} + (N^2_{1,2} - s^2)^{1/2}\,]^{1/2} \quad (II.11)$$

Where $N_{1,2}$ can be obtained using the following relation:

$$N_{1,2} = \frac{2s(T_M - T_{m1,2})}{T_M T_m} + \frac{s^2+1}{2} \qquad \text{(II.12)}$$

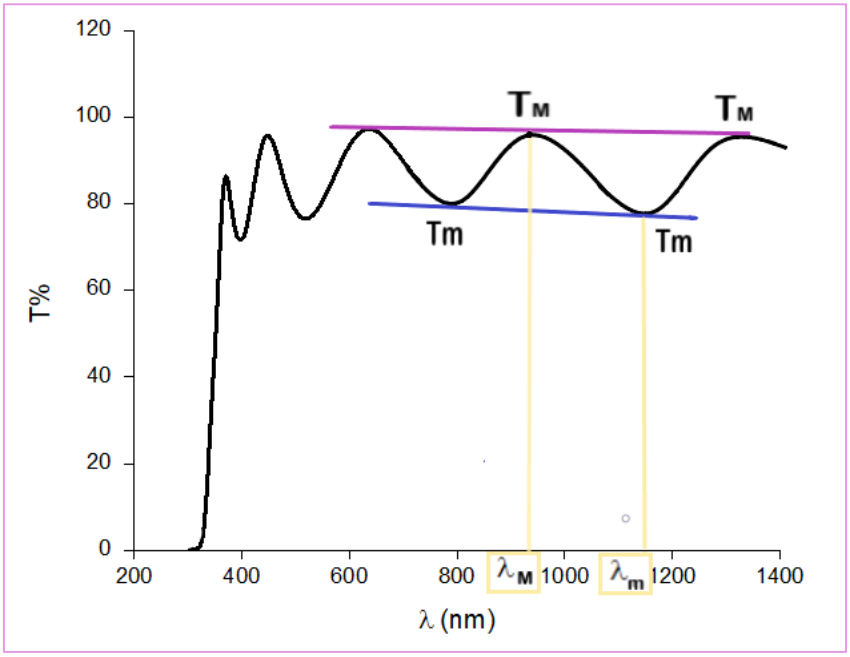

Figure II. 14. Transmittance spectra of TiO_2 thin films.

➢ **The second method**

The gravimetric method of weight difference estimates the thickness (t), taking into account the density (ρ) of TiO_2, which equals 3.78 g/cm^3. It has been defined by the following equation **[51]**:

$$d = \frac{\Delta m}{A\rho} \qquad \text{(II.13)}$$

Where:

- **d**: the thickness of the layer.
- **Δm**: the difference in masses (before and after) of the deposits.
- **ρ:** the density of TiO_2.
- **A**: the surface area of the thin layer.

II.3.3.3. Optical band gap (E_g)

The band gap energy is one of the important optical constants, as its value appears in some optical properties and disappears in others**[37]**. The equation linking the absorption coefficient (**α**) and the band gap energy ($\mathbf{E_g}$)is given by the following relationship **[9]**:

$$(\alpha h\nu)^n = A(h\nu - E_g) \qquad \text{(II.14)}$$

Where:

$h\nu$: the photon energy(eV).

E_g : optical band gap (eV).

n and A: constants.

α :the absorption coefficient.

n: characterizes the optical type of transition and takes the values 2, 1/2 (2 for allowed direct transitions or 1/2 for allowed indirect transitions)**[12]**.

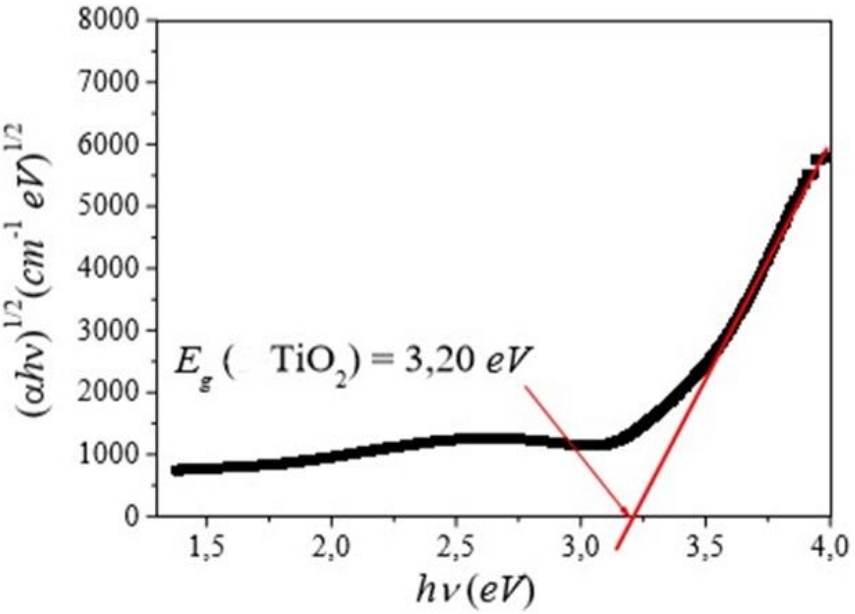

Figure II. 15. Plot (αhν)^(1/2) as a function of hν **[52]**.

II.3.3.4. Urbach energy (E_u)

Urbach energy (E_u) is computed to discern the state of material disorder in exploring optical characteristics. Urbach's law determines the absorption coefficient through the equation **[34]**:

$$\alpha=\alpha_0 \exp\left(\frac{h\nu}{E_u}\right) \qquad \text{(II.15)}$$

So, the value of Eu is determined by plotting lnα against hν as in the equation **[34]**:

$$\mathrm{Ln}(\alpha)=\mathrm{Ln}(\alpha_0)+\frac{h\nu}{E_u} \qquad \text{(II.16)}$$

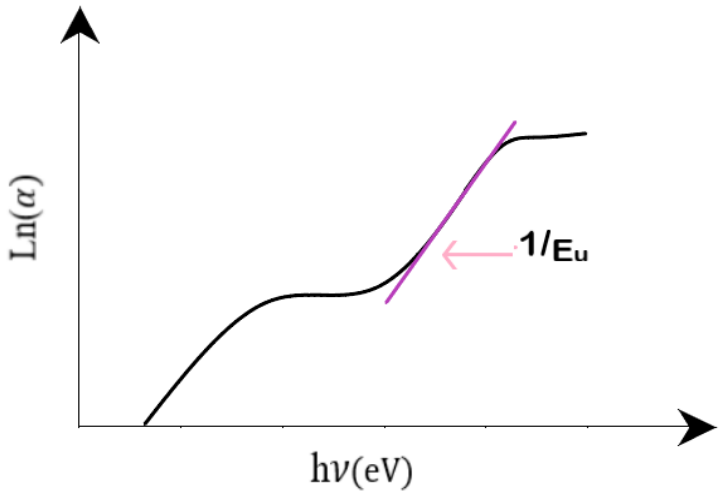

Figure II.16. Plot of Ln(α) as a function of hν.

II.3.4 electrical properties

- **The four-point method**

The study of conductivity has increased as a result of the widespread usage of thin films as resistors, contacts, and connectors. And it is significant from a theoretical and practical perspective. The four-point probe approach is the most often used technique for determining resistivity. The probes are separated equally. The outer two probes get a tiny current I from a constant-current source, and the voltage V between the inner two probes is then measured. This is accomplished by applying four spots on the sample's surface, spaced S apart, with equal pressure. By this technical, it is shown that in the case of thin films, expressed in Ω and hence deducing resistivity **ρ** (expressed as Ω.cm) are given through relationship **[53].**

$$\rho = R_{sheet} * d \qquad \text{(II. 17)}$$

Based on previous considerations, we deduce the formula to calculate the conductivity

$$\sigma = \frac{1}{\rho} \qquad \text{(II.18)}$$

Where:

d: the thickness of the layer. **ρ** = the resistivity (Ω.cm).

$\mathbf{R_{sheet}}$ = the square resistance ($\mathbf{R_{sheet}}=\frac{\pi u}{ln2.I}$, where,**U** is the voltage and **I** is the current)

II.3.5. morphological properties

- **Scanning electron microscopy (SEM)**

The morphological and compositional analysis of material surfaces can be conducted using a scanning electron microscope (SEM). Various signals can provide details about properties at and near a specimen's surface through electron interactions. Electrons scattered at angles greater than 90 degrees are particularly valuable. Secondary electrons, resulting from inelastic collisions of incident electrons with specimen electrons, are utilized to reveal surface structure with a resolution of approximately 10 nanometers or better **[54]**.

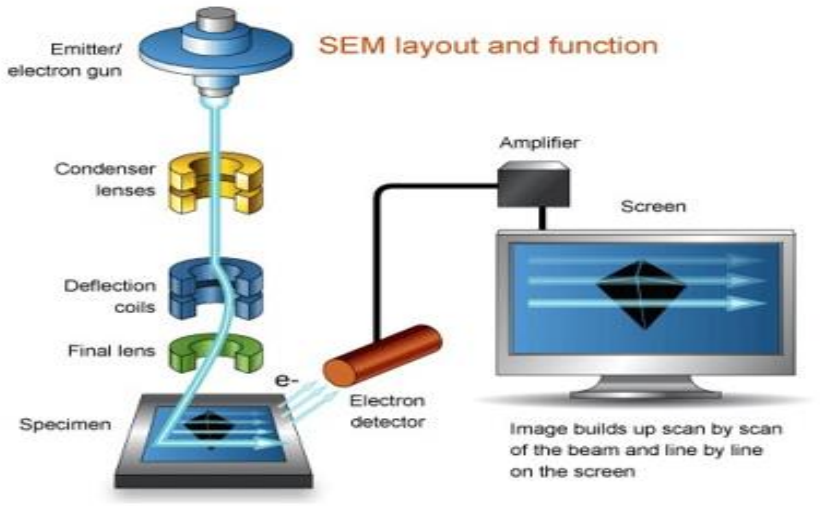

Figure.II.17. All scanning electron microscope (SEM) components **[55]**.

Chapter III

Thin films: Deposition and Analysis of results.

This chapter discusses the materials used in the experiment, their quantities, and the preparation method using the spin coating technique, as well as the steps to prepare the sol-gel solution. Additionally, the spin coating technique will be explained along with how it is applied to ensure the formation of homogeneous layers. Finally, the prepared films will be described using UV spectroscopy to determine optical properties and X-ray diffraction (XRD) to analyze the crystal structure and calculate physical parameters. The thin films were also described by the SEM.

III.1. Experimental procedures

III.1.1. Solutions used in the deposition process.

To prepare the solution intended for synthesizing TiO_2 thin films, three compounds are essential and each playing a crucial role in the composition and homogeneity of solution: the precursor, the solvent, and the catalyst.

III.1.1.1. Titanium Tetra-Isopropoxide (Precursor)

The quality of films produced by the sol-gel method is highly dependent on the properties of the precursors employed. These precursors must have good reactivity with the surface they contact. Additionally, the precursors must be thermally stable at the deposition temperature to achieve uniform surface saturation. This study uses titanium tetra-isopropoxide ($Ti[OCH(CH_3)_2]_4$) (TTIP) as the organometallic precursor for preparing the TiO_2 deposition solution via the spin coating method **[37]**. The properties of this precursor are detailed in **figure III.1**.

Figure III.1. The properties of Titanium Tetra-Isopropoxide.

III.1.1.2 Ethanol (solvent)

Alkoxides (such as titanium isopropoxide) are not miscible in water. Therefore, analcoholic solvent must be used to this mixture. It is preferable to use **ethanol**, as it corresponds to the –OR of the

alkoxide, to avoid potential reactions between the different components that could alter reaction kinetics**[37]**. The properties of ethanol in **figure III.2**.

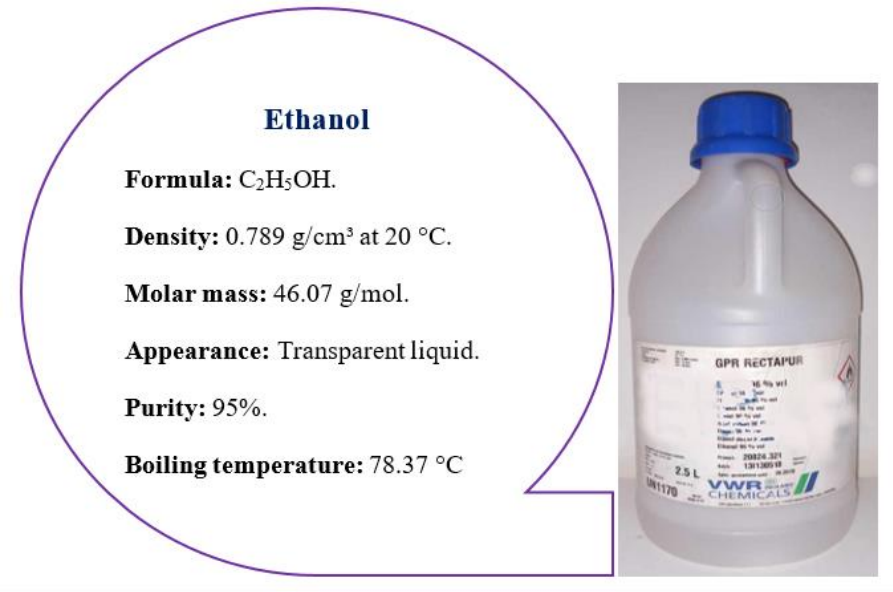

Figure III.2. The properties of Ethanol.

III.1.1.3. Acetylacetone (catalyst)

Acetylacetone (AcAc) is a very effective catalyst for TTIP **[37]**. The properties of acetylacetone in **figure III.3**.

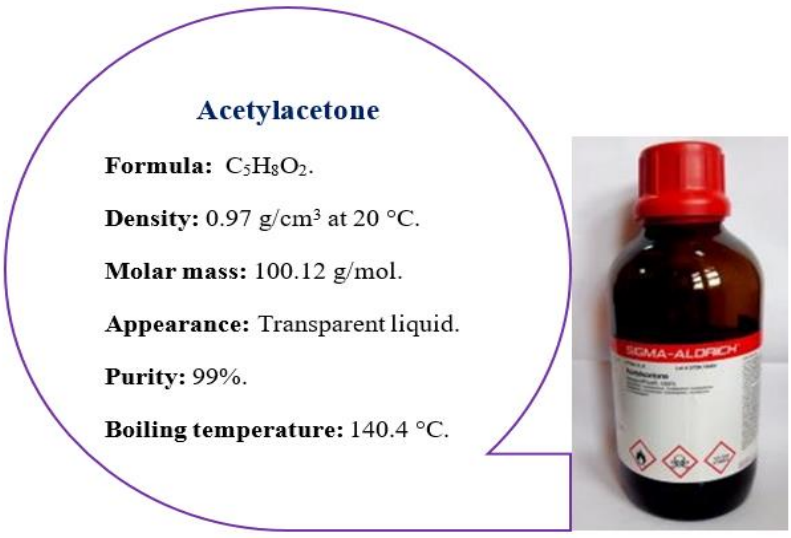

Figure III.3. The properties of Acetylacetone**.**

III.1.1.4. Lithium (doping element)

We have chosen lithium as a doping material that has never been tried on titanium oxide in our laboratory due to factors that we mentioned in the first chapter, such as the properties of the lithium used in the experiment.

Figure III.4. The properties of Lithium**.**

III.1.2. Preparation of Solution

III.1.2.1. Materials and Concentrations:

- Precursor: Titanium tetra-isopropoxide (TTIP) of 0.2%.
- Solvent: 10 mL of ethanol.
- Catalyst: AcAc at a concentration of 0.2%.
- Doping element: Li concentrations of 0at. %, 0.5at. %, 1at. %, 1.5at. %, and 2at.%.
- Both AcAc and TTIP have a molarity of (1:1).

III.1.2.2. Procedure

For the preparation of the deposition solution with a concentration of 0.2 mol/l, titanium tetra-isopropoxide (TTIP) used as a precursor is dissolved in ethanol with acetylacetone, lithium chloride (LiCl) was used as a doping source at (0, 0.5, 1, 1.5, 2 at.%). The resulting mixture is stirred with a magnetic stirrer at a temperature equal to 50° C for 3 hours. The molar ratio of acetylacetone (stabilizer) and TTIP equals 1. The final solution is transparent yellowish in color and slightly viscous (**Figure.III.5**).

Figure.III.5. The deposit solution.

III.1.3. Preparing the substrate.

III.1.3.1. Selection of Substrate for Deposition Solution

When selecting a substrate for a deposition solution, it is crucial to consider the physical and chemical properties of the solution under study. The aim is to avoid any potential reactions that may occur, ensuring optimal adhesion to the substrate. The conditions to be considered:

- optical properties :its transparencymakes it perfect for analyzing the optical properties of the films within the visible spectrum.
- Chemical Compatibility: the substrate should be inert chemically to prevent reactions from compromising.
- Surface Energy: Substrate surface energy should match the solution for better adhesion and uniform deposition.
- Thermal Stability: Substrate must withstand deposition process heat without deformation.
- Mechanical Properties: The substrate needs sufficient strength to support the deposited layer.
- Surface Roughness: Substrate surface roughness helps proper material growth.
- And, of course, they are available and less expensive.
- These considerations ensure a successful deposition process and high-quality deposits.

III.1.3.2. Cleaning of the substrates

The process for cleaning the substrates is as follows:

- Rinse with distilled water.
- Cleaning with acetone for 5 min to remove grease.
- Rinse with distilled water for 5 min
- Cleaning with alcohol for 5 min.
- Rinse with distilled water for 5 min.
- Drying using a dryer.

Cleaning substrates is an important procedure to avoid any contamination affecting electrical and optical proprieties.

Figure III.6. Glass Substrates and Diamond-Tipped Pen.

III.1.4. Thin film deposition

Following the solution preparation stage, the deposition process was conducted using a spin-coating device to obtain a layer with specific properties. The following steps were followed for each sample (**0%**, **0.5at%**, **1at%**, **1.5 at%**, **2 at%**):

- Place the glass substrate on the spinor support.
- Apply drops of the solution onto the glass substrate by a syringe.
- Activate the vacuum switch first to secure the glass substrate, then close the device.
- Turn on the rotation for **30** seconds at a constant speed of **400 rpm**.

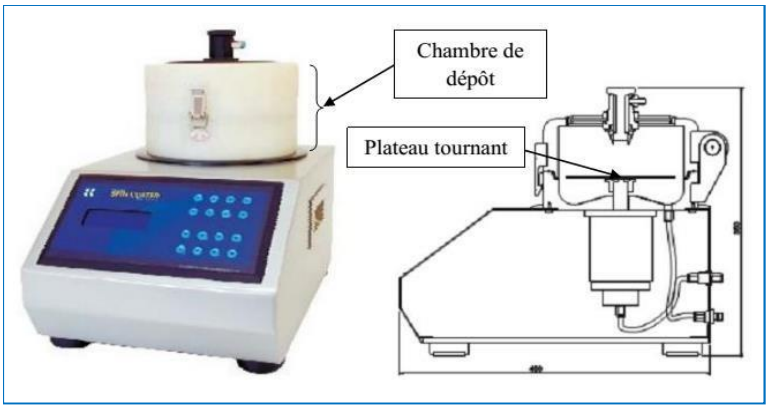

Figure III.7. Holmarc spin-coating

Following these stages, two essential phases of heat treatment ensure:

- **Drying of thin films**

After removing the sample, place it in an oven at **250°C** for **10** minutes. It corresponds to the evaporation of remaining solvents on the substrate surface.

Repeat the experiment **5** times to obtain the desired layer.

- **Annealing of thin layers**

The material is achieved through annealing in a resistance furnace at 600°C for 2 hours. This step is crucial for reaching the desired state. (**as shown in Figure III.8**)

Figure III.8. Annealing furnace.

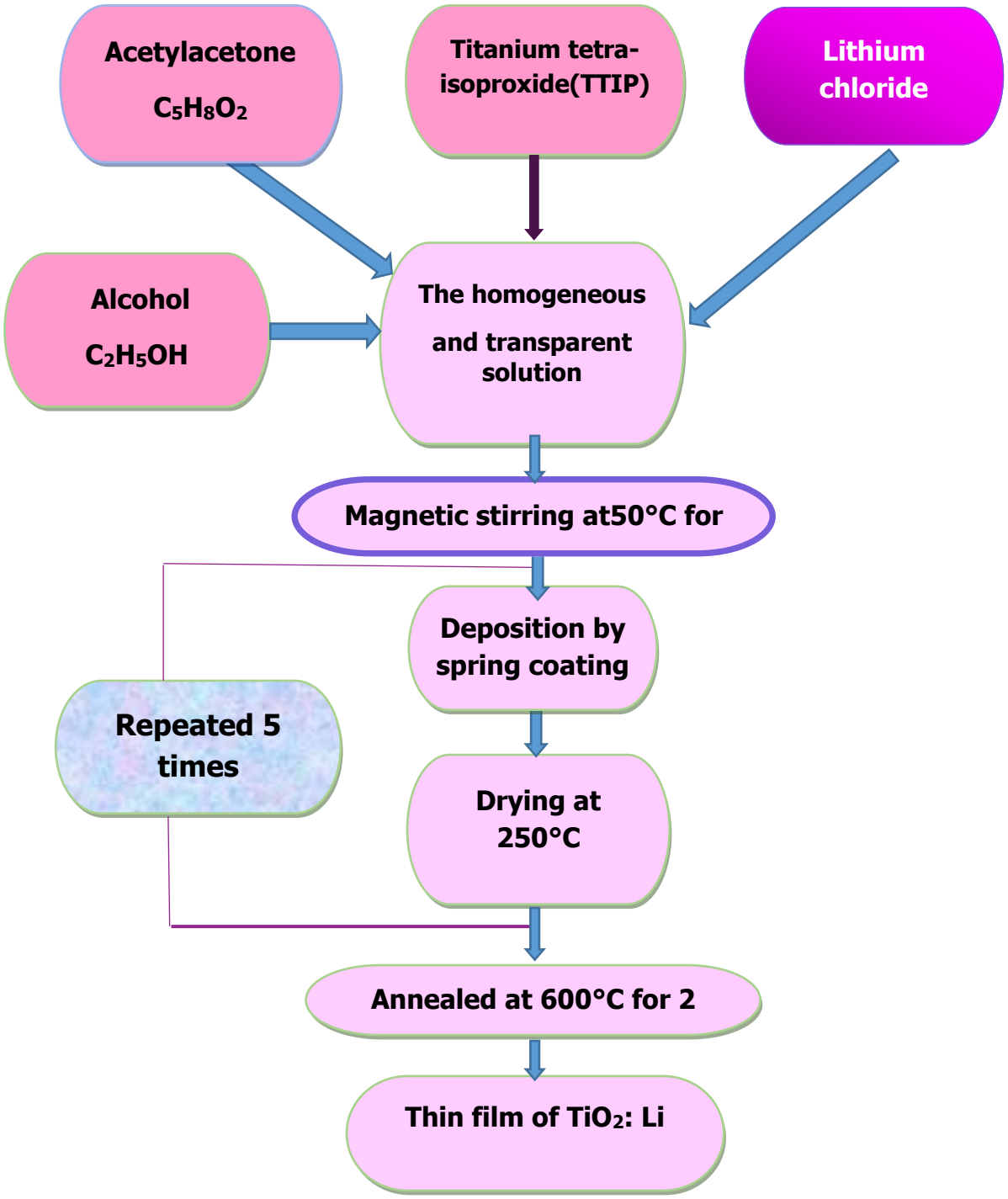

Figure III.9. A diagram summarizing the steps followed for the deposition of lithium-doped titanium oxide solution .

III .2 Results and discussions

III.2.1 Structural characterizations.

III.2.1.1. X-Rays diffraction.

In this study, the DRX (X-ray Diffraction) device was employed to analyze the crystalline structure of titanium dioxide and obtain the Miller indices of our layer planes by the ASTM sheet of Titanium Oxide in the anatase phase shown in the following (**figure III.10**).

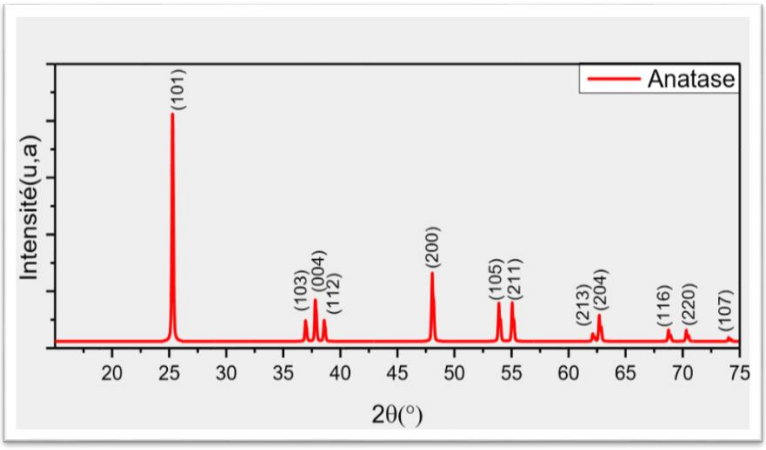

Figure III.10. X-ray diffraction spectrum (ASTM data sheet) of TiO_2 powder for Anatase **[56]**.

The different peaks characteristic of the TiO_2 structure for various Lithium concentrations are grouped in the (figure **III.10**).

Figure.III.10. shows the X-ray diffraction spectrum of TiO_2 thin film at different Li doping concentrations (0 at. %, 0.5 at%, 1 at. %, 1.5 at%, 2 at%) deposited on glass substrate at annealing temperature 600°C for 2 hours.

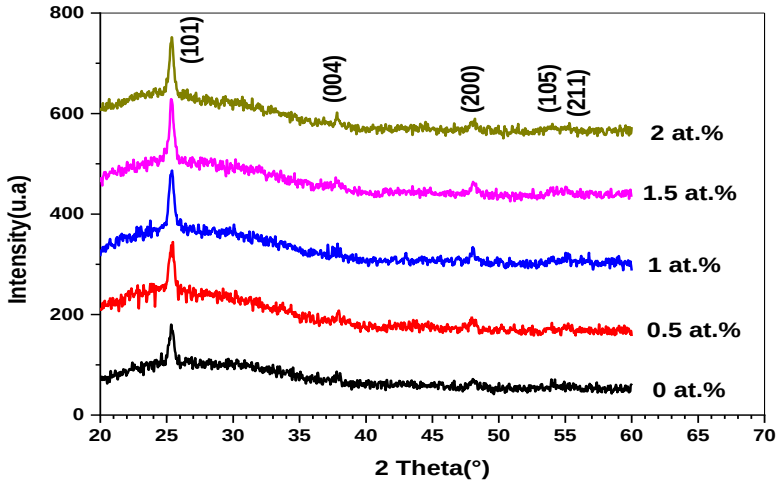

Figure.III.11. X-ray diffraction patterns for Li-doped TiO_2 thin films.

As can be seen, all the samples exhibited diffraction peaks with directions (101), (004), (200), (105), and (211), these peaks correspond to the anatase phase (tetragonal structure) and are in good agreement with those given in the ASTM sheets (ICCD No.21-1272). Following this figure, one can also notice that for pure and Li-doped TiO_2 thin film, the most intense peak was at the (101), which corresponds to the diffraction angle of about $2\theta = 25.36°$which can be related to the minimum energy for the growth of our thin films. Similar results were obtained by R.mchamess et al**[37]**, M.Dahnoun et al**[4]**, and A.El Bendali et al **[54]**. Furthermore, we also notice that the intensity of all peaks increases with Li doping concentration increase up to 1.5 at% then decreases at 2 at.%. These increases can be attributed to the incorporation of Li doping in the TiO_2 lattice.

III.2.1.2. Crystallite size, dislocation density, and micro-strain

To calculate the structural parameters using the equations (II.5), (II.6), and(II.7), mentioned in Chapter II**.**

The results are presented in the following table (III.2) and figure (III.11), we estimated from the highest peak (101) for all various samples. As can be seen, the crystallite size changes Inversely with both dislocation density and micro-strain with Li doping increases. On the other hand, we note that the increase in crystallite sizes related to the decreases in micro-strain leads to a decrease in grain boundaries.

Table III.1. The variation of Crystallite size and deformation according to doping.

Li (at.%)	**Crystallite size (nm)**	**Micro-strain ($\varepsilon \times 10^{-3}$)**	**Dislocation density ($\delta \times 10^{15}$)(line/m^2)**	**Intensity of the peak (101) (a.u)**
0	20,88	1,65939	2,29198	**76.75**
0.5	18,10	1,91469	3,05145	**95.42**
1	18,94	1,82959	2,78624	**126.15**
1.5	22,01	1,5743	2,06293	**129.07**
2	23,27	1,4892	1,84594	**117.67**

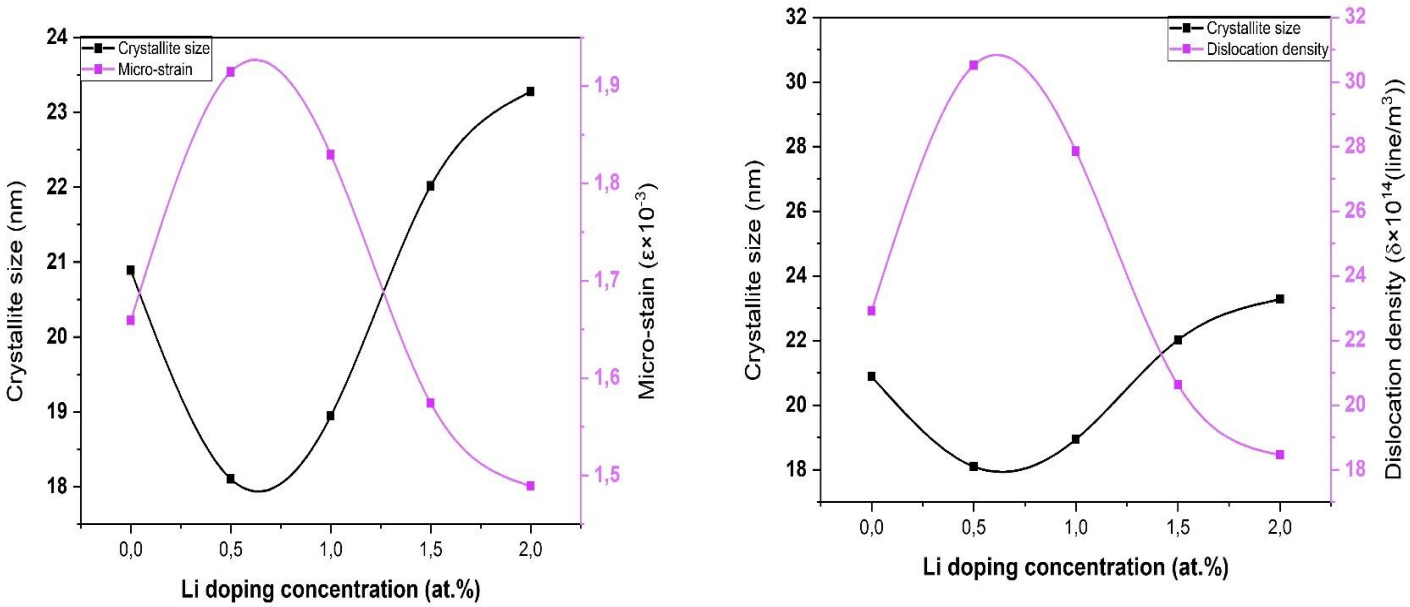

Figure.III.12. the variation of micro-strain and dislocation density with crystallite size as a function of lithium doping concentration.

III.2.2. Optical characterization measurements

III.2.2.1. Transmittance and reflectance spectra

Figure III.11 and Figure III.12illustrate the transmittance and reflectance spectra of titanium dioxide (TiO_2) thin films grown at various Li doping concentrations in the wavelength range of 290–1200 nm.

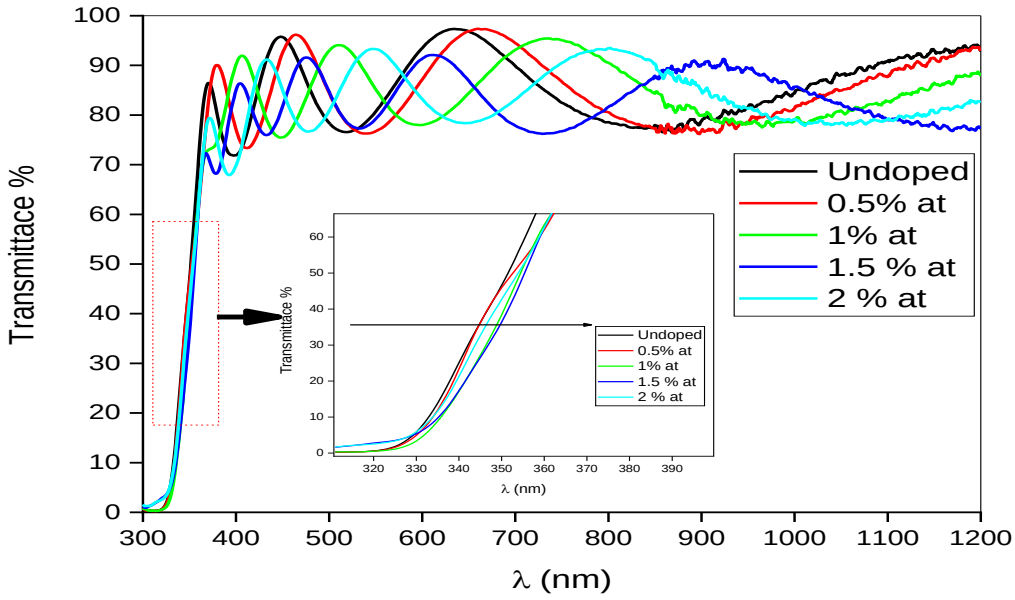

Figure III.13. The optical transmittance spectra of TiO_2 thin films at various Li doping concentrations.

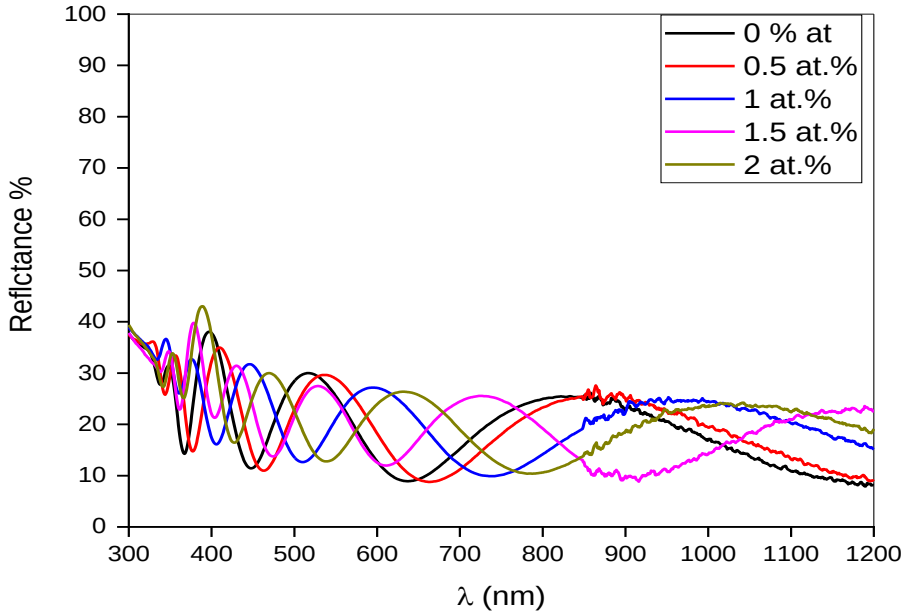

Figure III.14. The reflectance spectra of TiO_2 thin films at various Li doping concentrations.

Based on the information presented in (Figure III.13), it is evident that the transmittance spectra can be divided into two regions:

The first region demonstrates a significant level of transmittance within the wavelength spectrum ranging from 400 to 1200 nm. It is noteworthy to observe that all samples showcase a notable optical clarity of approximately 87% in the visible light spectrum, while the reflectance values are consistently confined within a narrow of approximately 19%.

The most samples exhibit interference fringes in both reflectance and transmission spectra within the visible region. This occurrence is likely due to the uniform surface of the films, A.Attaf et al **[57]**, O.Benkhettaet al **[58]**.

The second region exhibiting pronounced absorption features is associated with the primary absorption occurring at wavelengths less than 400 nm. This particular region is linked to the process wherein the transition of an electron from the valence band (BV) to the conduction band (BC) **[59]**. On the other hand, as the concentration of Lithium doping increases, the absorption edge of the deposited films shifts towards the higher wavelength spectrum (red shift), consequently leading to a decrease in the band gap energy. also, the higher transmittance observed in the films was attributed to less scattering effects.

III.2.2.2. Optical gap energy E_g and Urbach energy E_u

The energy band gap (Eg) and Urbach energy are important parameters in the photovoltaic application, which describes the optical behavior of transparent materials with light. These parameters were calculated from equations mentioned in Chapter II (**see Figure III.15 and Figure III.16**).

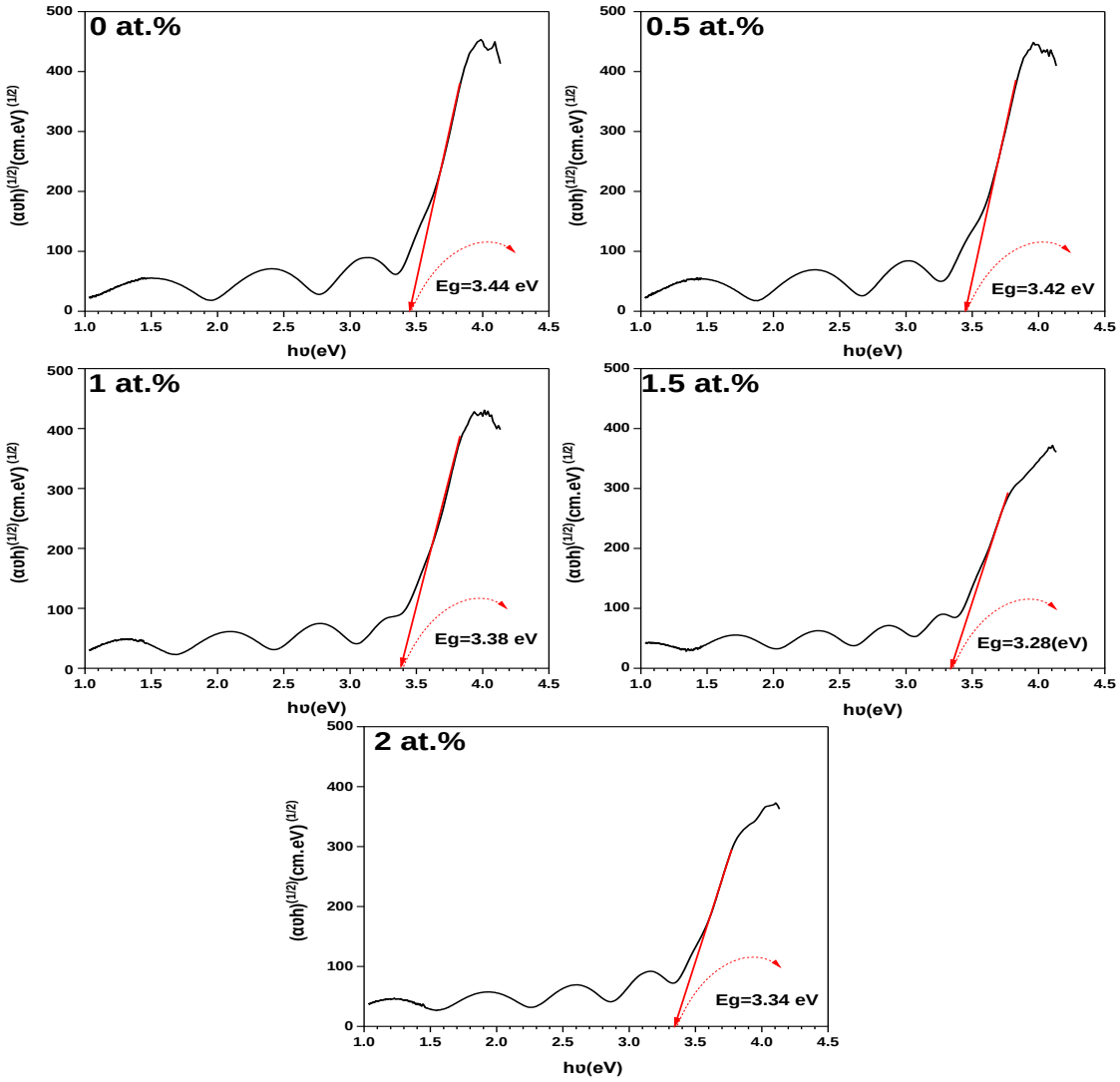

Figure.III.15. the variation of gap energy as a function of lithium doping concentration.

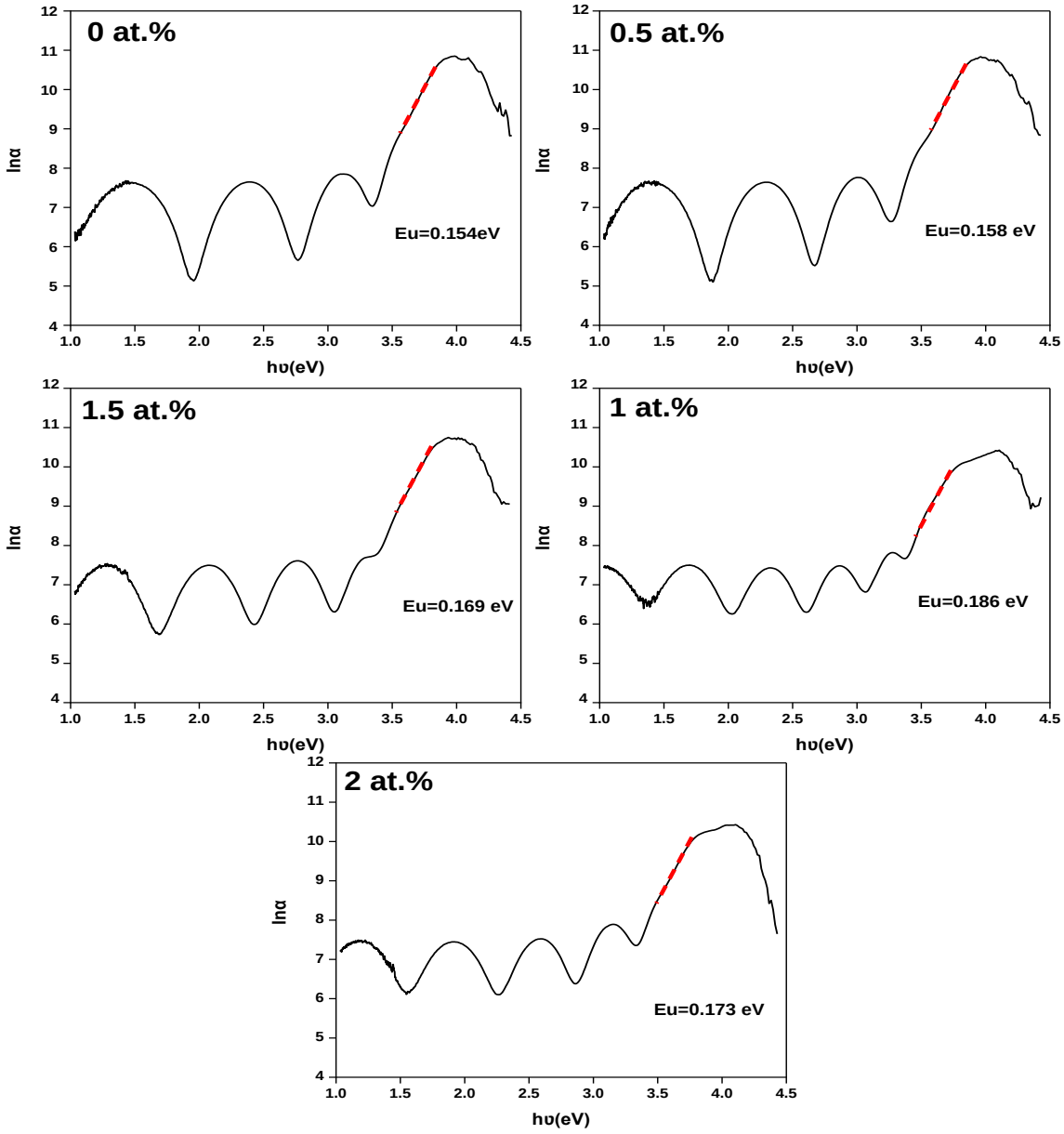

Figure.III.16. the variation of the Urbach energy as a function of lithium doping concentration.

As can be seen in **Table III.2** and **Figure III.17**, we noted that the band gap and the Urbach energies are inversely aligned. The Urbach tail width or energy is used as a signature of the disorder in the film lattice by Lithium doping concentration **[60].** Furthermore, it can be seen that band gap is going through two ranges as a function of Lithium doping concentration:

Low doping ranges from 0 to 1.5 .at% Li:

It can be seen that depending on the increasing Li doping concentration, the band gap values decreased from 3.44 eV to 3.28 eV. This decrease is interpreted as the doping leading to the formation of new localized states below the transport band. These states are prepared to accept electrons and generate

tails in the energy band gap, thus reducing it **[61]**. In addition, this decrease in the band gap has been attributed to the shrinkage effect, which is frequently observed in n-type semiconductors. While doping, the shrinkage of the band gap energy was due to the induced shifting of the conduction band minimum and valence band maximum **[39]**. The higher doping range is above 1.5 to 2 at.%. At Li: in this range, the band gap value increased from 3.28 eV to 3.33 eV. The increase in E_g is explained by the basis of the Burstein–Moss (BM) effect, an energy band widening effect resulting from the increase in the Fermi level in the conduction band of degenerated semiconductors. In another way, based on the Burstein-Moss effect, the increase in the carrier's density of semiconducting material due to Lithium doping causes a shift in the Fermi level and merges into the conduction band which causes the low energy transition is obstructed. This result is in good agreement with the results of Boean Houng et al **[55].**

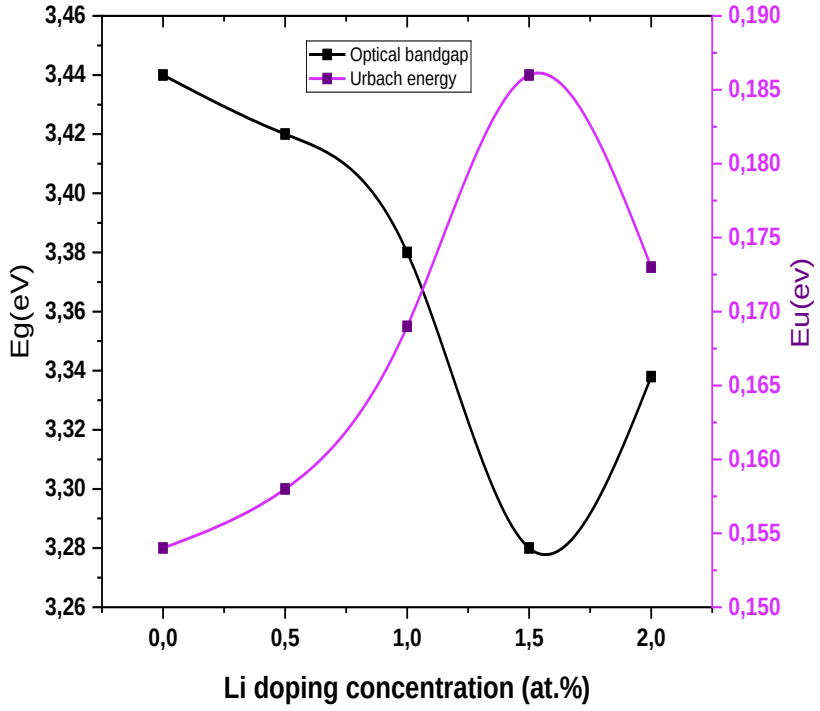

Figure.III.17. The variation of gap energy and the Urbach energy as a function of lithium doping concentration.

Following table III.2. Summarize the variation of E_g and E_u respectively:

Table III.2. The variations of average transmittance, average reflectance, gap energy, and the Urbach energy as a function of lithium doping concentration.

Li (at.%)	Average transmittance (%)	Average reflectance (%)	gap energy (eV)	Urbach energy (eV)
0	**86.67**	**19.36**	**3,44**	**0,154**
0,5	**86.87**	**19.07**	**3,42**	**0,158**
1	**87.03**	**18.84**	**3,38**	**0,169**
1,5	**82.67**	**21.30**	**3,28**	**0,186**
2	**85.04**	**19.91**	**3,33**	**0,173**

III.2.3. The thickness of the film

To calculate the film thickness (d) we used the method of interference fringes (Swanepoel's method) which was mentioned in the second chapter (equation II.10), the obtained results are represented in the table below.

Table III.3. The variation of thickness (d) with the lithium doping concentration.

Li (at.%)	0	0.5	1	1.5	2
d(nm)	**499**	**512**	**545**	**603**	**563**

we note that the film thickness values are almost converging. So, the effect of Lithium doping concentrations didn't significantly affect film thickness, but it clearly affected the structure of our samples. Also, this convergence of values refers to the sol-gel technical (spin coating) used in the sample preparation.

III.2.4. Surface morphology

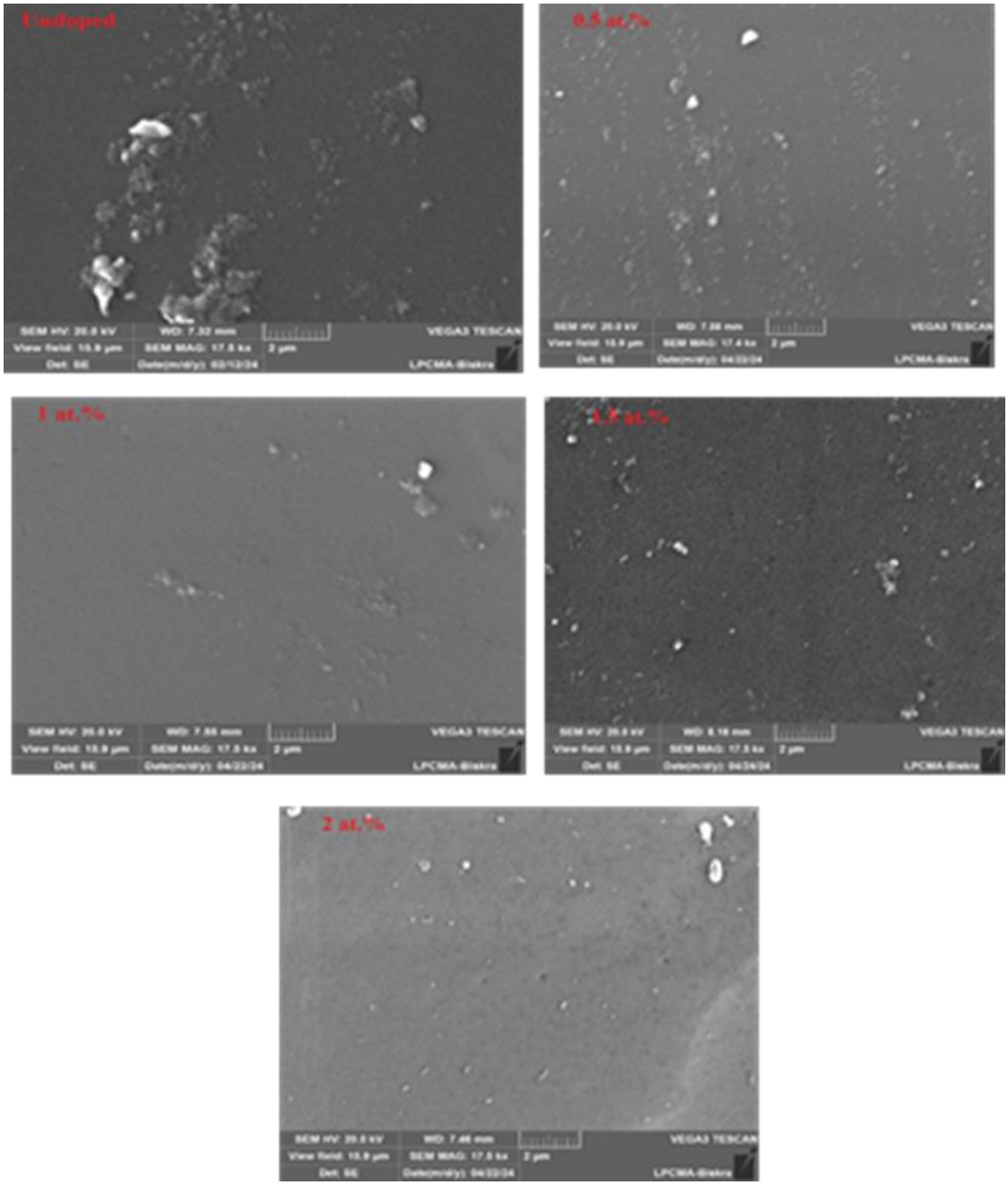

Figure III.18.SEM surface images of the TiO_2 thin films deposited at various doping concentrations.

Lithium doping effect on the morphological properties of TiO_2 thin films was investigated by scanning electron microscopy (SEM), shown in **Fig.III.18**. As the doping content increases, changes in the morphology of the films are observed. It is interesting to note, that the surface morphology of the samples generally revealed that the films are homogenous, smooth granular surfaces, continuous, dense,

and have some agglomerations. In the case of the films deposited at **2 at. %**, it is observed some pinholes ,which leading a deterioration in crystallinity this confirmed the results of DRX.

GENERAL CONCLUSION

The work presented in this study focused on the elaboration and characterization of Lithium doped Titanium dioxide TiO_2 thin films obtained by a sol-gel process (Spin-coating). The effect of doping on the structural, optical, and morphological properties of TiO_2 thin films was studied.

For this purpose, a series of five samples deposited on glass substrates with different concentrations (between 0% and 2%) were prepared and Titanium Isopropoxide as precursor, ethanol as solvent, Acetylacetone as stabilizer, and Lithium chloride as source of dopant.

And then we characterized our samples by the following techniques: X-Ray diffraction for structural properties, UV-Visible for optical characterization and finally SEM for morphology properties.

X-ray analysis showed that both doped and undoped titanium dioxide thin films crystallize with the tetragonal structure of the anatase phase with a preferential orientation(101)with doping concentrations of %1.5exhibiting the highest crystallinity. The size of the crystals was calculated, with the high-intensity peak at a value of 23.27 nm for 2 %doping, and the micro-strain values changed inversely with crystal size.

UV-visible spectroscopy analysis revealed that the doped and undoped titanium dioxide thin films exhibited high transmittance of up to 87%.In addition, we observed a shift towards longer wavelengths at the absorption edge. This technique was also utilized to calculate the band gap of the prepared thin films, indicating a decrease from 3.44 eV to 3.28 eV and an increase in the Urbach energy from 0.154 eV to 0.186 eV.

An SEM image of doped and undoped titanium dioxide thin films revealed that the films are homogenous, smooth granular surfaces, continuous, dense, and have some agglomerations.

From the results obtained, it can be said that the elaborate thin films can be used in several applications such as photo-catalysts, optical windows, and gas sensors.

Our perspectives are to improve the electrical properties of TiO_2 thin films to make them applicable in photovoltaic fields by using for example: Other doping or Co-doping.

Annex

ASTM sheets for the TiO_2 anatase phase

Name and formula

Reference code:	00-021-1272
Mineral name:	Anatase, syn
Compound name:	Titanium Oxide
PDF index name:	Titanium Oxide
Empirical formula:	O_2Ti
Chemical formula:	TiO_2

Crystallographic parameters

Crystal system:	Tetragonal
Space group:	I41/amd
Space group number:	141
a (Å):	3,7852
:b (Å)	3,7852
:c (Å)	9,5139
:(°) Alpha	90,0000
:(°) Beta	90,0000
:(°) Gamma	90,0000
:Calculated density (g/cm^3)	3,89
:Volume of cell (10^6 pm^3)	136,31
:Z	4,00
:RIR	3,30

Subfiles and quality

Subfiles:	Alloy, metal or intermetalic
	Common Phase
	Corrosion
	Educational pattern
	Forensic
	Inorganic
	Mineral
	NBS pattern
	Pharmaceutical
	Pigment/Dye
Quality:	Star (S)

Comments

Color:	Colorless
Creation Date:	01/01/1970
Modification Date:	01/01/1970
Color:	Colorless
Additional Patterns:	See ICSD 9852 (PDF 01-071-1166)

Sample Source or Locality: Sample obtained from National Lead Co., South Amboy, New Jersey, USA. Anatase and another polymorph, brookite (orthorhombic), are converted to rutile (tetragonal) by heating above 700 C. Pattern reviewed by Holzer, J., McCarthy, G., North Dakota State Univ, Fargo, North Dakota, USA, ICDD Grant-in-Aid (1990). Agrees well with experimental and calculated patterns Additional Patterns: Validated by calculated pattern Temperature of Data Collection: Pattern taken at 25 C.

References

Primary reference: Natl. Bur. Stand. (U.S.) Monogr. 25,) ,82 ,71969(

Peak list

No. h k l d [A] 2Theta[deg] I [%]

1	1	0	1	3,52000	25,281	100,0
2	1	0	3	2,43100	36,947	10,0
3	0	0	4	2,37800	37,801	20,0
4	1	1	2	2,33200	38,576	10,0
5	2	0	0	1,89200	48,050	35,0
6	1	0	5	1,69990	53,891	20,0
7	2	1	1	1,66650	55,062	20,0
8	2	1	3	1,49300	62,121	4,0
9	2	0	4	1,48080	62,690	14,0
10	1	1	6	1,36410	68,762	6,0
11	2	2	0	1,33780	70,311	6,0
12	1	0	7	1,27950	74,031	2,0
13	2	1	5	1,26490	75,032	10,0
14	3	0	1	1,25090	76,020	4,0
15	0	0	8	1,18940	80,727	2,0
16	3	0	3	1,17250	82,139	2,0
17	2	2	4	1,16640	82,662	6,0
18	3	1	2	1,16080	83,149	4,0
19	2	1	7	1,06000	93,221	2,0
20	3	0	5	1,05170	94,182	4,0
21	3	2	1	1,04360	95,143	4,0
22	1	0	9	1,01820	98,319	2,0
23	2	0	8	1,00700	99,804	2,0
24	3	2	3	0,99670	101,221	2,0
25	3	1	6	0,95550	107,448	4,0
26	4	0	0	0,94640	108,963	4,0
27	3	0	7	0,92460	112,841	2,0
28	3	2	5	0,91920	113,861	2,0
29	4	1	1	0,91380	114,909	2,0
30	2	1	9	0,89660	118,439	4,0
31	2	2	8	0,88900	120,104	2,0
32	4	1	3	0,88190	121,725	2,0
33	4	0	4	0,87930	122,336	2,0
34	4	2	0	0,84640	131,036	2,0
35	3	2	7	0,83080	135,998	2,0
36	4	1	5	0,82680	137,391	4,0
37	3	0	9	0,81020	143,888	2,0
38	4	2	4	0,79740	150,039	4,0
39	0	0	12	0,79280	152,634	2,0

Stick Pattern

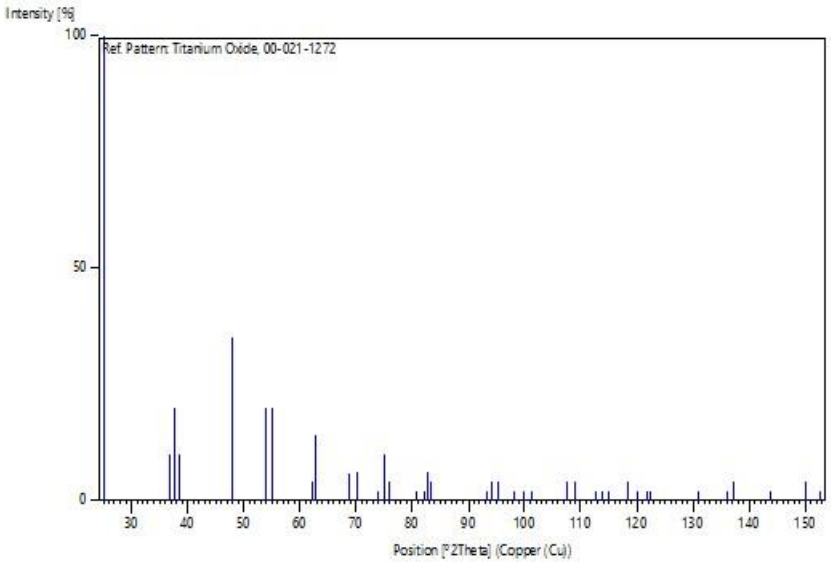

References

[1] Idris, M. M., Olarinoye, I. O., Kolo, M. T., & Ibrahim, S. O. (2022). Transparent conducting oxides thin film dosimetry: Present and the future.

[2] بتقنية الرذاذ الانحلال الحراري ,مذكرة ماستر ,جامعة قاصدي مرباح ورقلة ,2020.(zno) ن.قمو,ا.ميموني,<<دراسة و تحضير اغشية رقيقة لاكسيد الزنك النقي

[3] Hautier, G., Miglio, A., Ceder, G., Rignanese, G. M., & Gonze, X. (2013). Identification and design principles of low hole effective mass p-type transparent conducting oxides. Nature communications, 4(1), 2292.

[4] M.Dahnoun , <<Preparation and characterization of Titanium dioxide and Zinc oxide thin films via Sol-Gel (spin coating) technique for optoelectronic applications>>,doctoral dissertation, University Mohamed Khider of Biskra,(2019).

[5] F,ZERIBI,<< Elaboration and characterization of titanium dioxide thin films by Sol-Gel (spin - coating) process for photovoltaic applications>>, doctoral dissertation, University of Kasdi Merbah Ouargla,(2022).

[6] Xu, Y., & Zangari, G. (2021). TiO_2 nanotubes architectures for solar energy conversion. Coatings, 11(8), 931.

[7] N.DJEHAICHE,<< Effect of Niobium doping on the properties of Titanium Dioxide (TiO_2) Thin films elaborated by Sol-Gel (Spin-coating)>>, Master Dissertation, University Mohamed Khider of Biskra,(2018).

[8] N.Hamidi,<<Elaboration et caractérisation des couches minces d'oxyde de titane dopé Sn>>, UNIVERSITE MOHAMED SEDDIK BEN YAHIA of JIJEL,(2019).

[9] R. Ben atia,<< Elaboration et caractérisation des couches minces d'oxyde de titane (TiO_2) obtenue par procédé Sol-Gel : l'effet de la température du recuit>>, University Mohamed Khider of Biskra,(2015).

[10] K.ATAMNIA,<< Synthèse par voie sol-gel et caractérisation des gels d'oxydes de titane (TiO_2) nanostructurés: applications en photocatalyse>>, Université 8 Mai 1945 Guelma,(2018).

[11] O.HERIBI,<< Effect of PH precursor on properties of TiO_2 thin films deposited by ultrasonic spray process and their photocatalytic applications>>, University Mohamed Khider of Biskra,(2022).

[12] Jassal, P. S., Kaur, D., Prasad, R., & Singh, J. (2022). Green synthesis of titanium dioxide nanoparticles: development and applications. Journal of Agriculture and Food Research, 10, 100361.

[13] Seman, N., Tarmizi, Z. I., Ali, R. R., Taib, S. H. M., Salleh, M. S. N., Zhe, J. C., & Sukri, S. M. (2022, November). Preparation Method of Titanium Dioxide Nanoparticles and Its Application: An Update. In IOP Conference Series: Earth and Environmental Science (Vol. 1091, No. 1, p. 012064). IOP Publishing.

[14] y.bouachiba,<< contribution of titanium oxide laboratories using the sol-gel formula: effect of doping and experimental conditions », Constantine university, 2014.

[15] Karthik, K., Pandian, S. K., & Jaya, N. V. (2010). Effect of nickel doping on structural, optical and electrical properties of TiO_2 nanoparticles by sol–gel method. Applied Surface Science, 256(22), 6829-6833.

[16] ف. بوحفص ,خ.سعد الله,<< دراسة الخصائص الضوئية لألغشية الرقيقة ل كسيد النيكل(NiO (المطعم بأيونات الليثيوم>>, جامعة قاصدي مرباح ورقلة,(2021).

[17] Ahmad, F., Khalid, M., & Panigrahi, B. K. (2021). Development in energy storage system for electric transportation: A comprehensive review. Journal of Energy Storage, 43, 103153.

[18] Kamienski, C. W., McDonald, D. P., Stark, M. W., & Papcun, J. R. (2000). Lithium and lithium compounds. Kirk-Othmer Encyclopedia of Chemical Technology.

[19] Chemistry of Lithium (Z=3). (2018). In Chemistry (Zumdahl and Decoste), (p. 591). Retrieved fromhttps://chem.libretexts.org.

[20] م.براء الله,ن.دبة,<< تأثير درجة الحرارة على الخصائص الفيزيائية للطبقات الرقيقة لكسيد النيكل(NiO)>>,جامعة قاصدي مرباح ورقلة,(2017).

[21] L.,HERISSI,<< Élaboration par pulvérisation pyrolytique et caractérisation de couches minces semiconductrices et transparentes d'oxyde de zinc : Perfectionnement du système de dépôt>>,(2008).

[22] Bedikyan, L., Zakhariev, S., & Zakharieva, M. (2013). Titanium Dioxide Thin Films: Preparation and Optical Properties. Journal of Chemical Technology & Metallurgy, 48(6).

[23] Simon, J. C., Dauby, B., & Nonet, S. (2008). Evaluation de l'efficacité de l'oxydation avancée par photocatalyse hétérogène UV/TiO_2 sur un effluent industriel contaminé par des composés organiques non biodégradables (colorants). Revue scientifique des ISILF, 22, 18-20.

[24] Das, R., Ambardekar, V., & Bandyopadhyay, P. P. (2021). Titanium dioxide and its applications in mechanical, electrical, optical, and biomedical fields (Vol. 7). London, UK: IntechOpen.

[25] Hafiw ,M.(2022).Titanium Dioxide –Advancces and Applications.Saudi Arabia,King Fahd University of Petroleum and Minerals.

[26] M.BDIRINA,<< SYNTHESIS AND CHARACTERIZATION OF ZINC OXIDE THIN FILMS FOR THE OPTIMIZATION OF A SPRAY DEPOSITION SYSTEM>>, Memory Magister, University Mohamed Khider of Biskra,(2012).

[27] A.Shano Al-Askari ,<< Effect of Aqueous Solution Molarity on Structural and Optical Properties of Nickel- Cobalt Oxide Thin Films Prepared by Chemical Spray Pyrolysis Method>>, Memory Magister, University Diyala of Iraq,(2012).

[28] Venables , J. (2000). Introduction to surface and thin film processes. Cambridge university press.

[29] Chaudhari, M. N., Ahirrao, R. B., & Bagul, S. D. (2021). Thin film deposition methods: A critical

[30] ه.فقعاص, ذ.شعباني,<< تحضير و دراسة طبقات رقيقة من أكسيد النيكل (NiO)مطعم بالنحاس(cu), جامعة محمد الصديق بن يحيى – جيجل,(2022).

[31] Salehabadi, A., Enhessari, M., Ahmad, M. I., Ismail, N., & Gupta, B. D. (2023). Metal Chalcogenide Biosensors: Fundamentals and Applications. Elsevier.

[32] R.MESSEMCHE,<< Elaboration and characterization of undoped and doped titanium dioxide thin layers by sol gel (spin coating) for photocatalytic applications.>>, doctoral dissertation, University Mohamed Khider of Biskra,(2021).

[33] L.E. Scriven, C.J. Brinker, D.E. Clark, D.R. Ulrich, Better ceramics through chemistry III, Mat Res Soc, 1988.

[34] A.Yahia,<< Optimization of indium oxide thin films properties prepared by sol gel spin coating process for optoelectronic applications>>, doctoral dissertation, University Mohamed Khider of Biskra,(2019).

[35] Frederichi, D., Scaliante, M. H. N. O., & Bergamasco, R. (2021). Structured photocatalytic systems: photocatalytic coatings on low-cost structures for treatment of water contaminated with micropollutants—a short review. Environmental Science and Pollution Research, 28(19), 23610-23633.

[36] A.GUETTAF,<< L'effet du dopage par l'étain sur les propriétés des couches minces de TiO_2élaborées par voie sol-gel (sping-coating)>>, University Mohamed Khider of Biskra,(2017).

[37] R.MESSEMCHE,<< Caracterisation des couches minces doxyde de titan (TiO_2)optenue par sol-gel (spin coating) :Leffet de la concentration de la solution.>>, Master Dissertation, University Mohamed Khider of Biskra,(2016).

[38] Griffin, J., & O'Kane, M. (2020). Dip coating: practical guide to theory and troubleshooting.

[39] k.Ben Aissa,<< Deposition and characterization of Tin Oxide thin films prepared by ultrasonic spray: influence of the low flow rates of solution.>>, Master Dissertation, University Mohamed Khider of Biskra,(2015).

[40] Aronica, C., & Jeanneau, E. (2009, October 28). Diffraction des rayons X: Techniques et structures cristallines. Cultures Sciences Physique.

[41] Kann, S. (2013). X-Ray Diffraction by NaCl.

[42]ا.زنو<< دراسة الخصائص البنيوية و الضوئية لألفالم الرقيقة لـ TiO 2المحضرة بطريقة الـGel-So >>, مذكرة ماستر, جامعة قاصدي مرباح ورقمة,(2016).

[43] Trifoi, A. R., Matei, E., Râpă, M., Berbecaru, A. C., Panaitescu, C., Banu, I., & Doukeh, R. (2023). Coprecipitation nanoarchitectonics for the synthesis of magnetite: A review of mechanism and characterization. Reaction Kinetics, Mechanisms and Catalysis, 136(6), 2835-2874.

[44] C.Khelifi,<< Tin dioxide SnO2 thin films deposited by ultrasonic spray technique: Properties and Applications>>, Master Dissertation, University Mohamed Khider of Biskra,(2017).

[45] Rodríguez-Lazcano, Y., Pena, Y., Nair, M. T. S., & Nair, P. K. (2005). Polycrystalline thin films of antimony selenide via chemical bath deposition and post deposition treatments. Thin Solid Films, 493(1-2), 77-82.

[46] Sharma, U. K., & Shyma, M. S. <<UV-Visible Spectroscopy: Instrumentation>>. Department of Pharmaceutics, Mar Dioscorus College of Pharmacy.(2019).

[47] Epp, J. (2016). X-ray diffraction (XRD) techniques for materials characterization. In Materials characterization using nondestructive evaluation (NDE) methods (pp. 81-124). Woodhead Publishing.

[48] Yakuphanoglu, F., Cukurovali, A., & Yilmaz, I. (2004). Single-oscillator model and determination of optical constants of some optical thin film materials. Physica B: Condensed Matter, 353(3-4), 210-216.

[49] R.BARIR,<< Caractérisation Spectroscopique des Couches minces d'oxyde de Nikel (NiO) Elaborées par Spray>>, doctoral dissertation, University of Kasdi Merbah Ouargla,(2018).

[50] و.حمود فيحان,<<الاغشية الرقيقة>>, شهادة البكالوريوس,جامعة بابل,(2023).

[51] Y. Lu et al, Doping concentration effects upon column-structured TiO_2: Nb for transparent conductive thin films prepared by a sol-gel method, J. Alloys Compd., 663(2016), pp. 413– 418.

[52] B.Saadi,<< Synthèse et caractérisations d'oxyde semiconducteurs de type p en couches minces par chimie douce pour des applications photovoltaiques>>, doctoral dissertation, University Mohamed Khider of Biskra,(2024).

[53] C. Khelifi, A. Attaf, H. saidi, A. Yahia, and M. Dahnoun, Investigation of F doped SnO2 thin films properties deposited via ultrasonic spray technique for several applications, Surfaces and Interfaces, 15(2019), pp. 244–249.

[54] El Bendali, A., Aqil, M., Hdidou, L., El Halya, N., El Ouardi, K., Alami, J., ... & Dahbi, M. (2024). The Electrochemical and Structural Changes of Phosphorus-Doped TiO_2 through In Situ Raman and In Situ X-Ray Diffraction Analysis. ACS omega, 9(13), 14911-14922.

[55] Mohammed, A., & Abdullah, A. (2018, November). Scanning electron microscopy (SEM): A review. In Proceedings of the 2018 International Conference on Hydraulics and Pneumatics—HERVEX, Băile Govora, Romania (Vol. 2018, pp. 7-9).

[56] O.Benkhetta,<< Effet de la concentration de la solution sur les propriétés des couches minces de dioxyde de titane déposées par spray pyrolyse ultrasonique >>, Memiore de master, Université Mohamed Khider de Biskra,(2019).

[57] Attaf, A., Messemeche, R., Saidi, H., Youcef, B., Aida, M. S., & Benkhetta, O. (2023). Characterization and photocatalytic activity of different molar ratios of TiO 2 thin films prepared by Sol-Gel process. Main Group Chemistry, (Preprint), 1-11.

[58] Attaf, A., Derbali, A., Saidi, H., Bouhdjer, A., Aida, M. S., Messemeche, R., ... & Djehiche, N. E. (2022). Precursor concentration effect on the physical properties of transparent titania (Anatase-TiO_2) thin films grown by ultrasonic spray process for optoelectronics application. Optical Materials, 132, 112790.

[59] C.Saadia,<< L'effet de dopage par l'aluminium sur les propriétés des couches minces du TiO_2 élaborées par voie Sol-Gel (spin caoting)>>, Memiore de master, Université Mohamed Khider de Biskra,(2016).

[60] Mestres, M. G. (2010). Synthesis and characterization of optical nanocrystals and nanostructures. An approach to transparent laser nanoceramics. Universitat Rovira i Virgili.

[61] ع. جنم صاحل، أ . ابراهيم حسن، دراسة أتثري نوع وطبيعة أألرضية على اخلواص البصرية ألغشية(NiO(احملضر ة بطريقة الطالء الدوراين ،جملة تكريت للعلوم الصرفة ،العدد02- ،الرقم ،1 0212 ،.131-ص 106 ،.

The effect of Lithium doping on the properties of Titanium dioxide thin films elaborated by Sol-Gel (spin coating).

Abstract:

In this study, we deposited undoped and Lithium-doped titanium dioxide thin films with doping concentrations varied (0.5%, 1%, 1.5%, 2%) onto glass substrates using the sol-gel (spin coating) method. The influence of Li doping on structural, optical, and morphological properties was investigated and then characterized using X-ray diffraction, UV-visible spectroscopy, and Scanning Electron Microscopy (SEM).

X-ray analysis showed that both doped and undoped titanium dioxide thin films crystallize with the tetragonal structure of the anatase phase with a preferential orientation (101), with doping concentrations of 1.5% exhibiting the highest crystallinity. The size of the crystals was calculated, with the high-intensitypeak at a value of 23.27 nm for 2% doping, and the micro-strain values changed inversely with crystal size.

UV-visible spectroscopy analysis revealed that the doped and undoped titanium dioxide thin films exhibited high transmittance of up to 87%. In addition, we observed a shift towards longer wavelengths at the absorption edge. This technique was also utilized to calculate the band gap of the prepared thin films, indicating a decrease from 3.44 eV to 3.28 eV and an increase in the Urbach energy from 0.154 eV to 0.186 eV.

An SEM image of doped and undoped titanium dioxide thin films revealed that the films are homogenous, smooth granular surfaces, continuous, dense, and have some agglomerations.

In summary, the results demonstrate that doping titanium dioxide with lithium improves the material's properties and enhances its efficiency in various applications. The prepared slices exhibited optical properties, while electrical measurements were inconclusive due to the specific conditions required for measurement.

The study concludes that the sol-gel method is an effective technique for doping titanium oxide with lithium, and the produced slices possess physical and chemical properties suitable for a wide range of technical applications. Further studies are recommended to explore the potential for improving these materials' properties and practical applications.

The keywords:TiO_2, thin films, spin coating, doping, structural properties, and optical properties.

L'effet du dopage au lithium sur les propriétés des films minces de dioxyde de titane élaborés par sol-gel (dépôt par centrifugation).

Résumé :

L'oxyde de titane a été dopé au lithium à différentes ratios (0,5%, 1%, 1,5%, 2%) en utilisant la méthode sol-gel, qui est une technique innovante permettant la préparation de nanomatériaux aux propriétés structurale, optique et électronique. L'étude s'est concentrée sur la caractérisation des films minces en utilisant plusieurs techniques pour déterminer leurs propriétés physiques et chimiques.

L'analyse par rayons X a montré que le titane dopé et non dopé cristallise tous deux dans la structure tétragonale de la phase anatase avec une direction préférentielle de (101), le taux de dopage de 1,5% présentant une cristallinité plus élevée. La taille des cristaux a été calculée, avec un pic enregistré à une valeur de 23,27 nm pour un dopage de 2%, et les valeurs de distorsion ont changé de manière inverse avec la taille des cristaux

L'analyse spectroscopique UV-visible a révélé que le titane dopé présentait une transmittance élevée allant jusqu'à 87%, se déplaçant vers des longueurs d'onde plus longues au bord d'absorption. Cette technique a également été utilisée pour déterminer la bande interdite des tranches préparées, indiquant une diminution de 3,44 eV à 3,28 eV et une augmentation de l'énergie d'Urbach de 0,154 eV à 0,186 eV, suggérant une augmentation des défauts dans la structure.

En résumé, les résultats montrent que le dopage de l'oxyde de titane avec du lithium améliore les propriétés du matériau et renforce son efficacité dans diverses applications. Les tranches préparées présentaient des propriétés optiques, tandis que les mesures électriques étaient peu concluantes en raison des conditions spécifiques requises pour les mesures. L'étude conclut que la méthode sol-gel est une technique efficace pour le dopage de l'oxyde de titane avec du lithium, et les tranches produites possèdent des propriétés physiques et chimiques adaptées à un large éventail d'applications techniques.

Des études supplémentaires sont recommandées pour explorer le potentiel d'amélioration des propriétés de ces matériaux et de leurs applications pratiques.

Les mots-clés: TiO_2 , films minces, revêtement par centrifugation, dopage, propriétés structurales, propriétés optiques.

تأثير شوائب الليثيوم على خصائص أفلام أكسيد التيتانيوم الرقيقة المحضرة بتقنية السول-جل (الطلاء بالدوران).

ملخص :

تم تطعيم أكسيد التيتانيوم بواسطة الليثيوم بنسب مختلفة (0,5%;1%;1,5%;2%)باستخدام طريقة سائل هلام، وهي تقنية مبتكرة تمكّن من تحضير مواد نانوية ذات خصائص هيكلية ،ضوئية ،والكترونية. تركزت الدراسة على توصيف الشرائح الرقيقة باستخدام تقنيات متعددة لتحديد خصائصها الفيزيائية والكيميائية.

تحليل الأشعة السينية أظهر أن التيتانيوم المطعم وغير المطعم يتبلوران في التركيب الرباعي لمرحلة الأناتاز والاتجاه المفضل (101)، وكانت نسبة التطعيم% 1.5أكثر تبلورًا، وتم حساب حجم البلورات حيث سجلت ذروتها عند القيمة 23.27(nm)بتطعيم 2%، كما تتغير قيم التشوه بصورة عكسية لحجم البلورات.

التحليل الطيفي بالأشعة فوق البنفسجية أظهر أن أكسيد التيتانيوم المطعم وغير المطعمله متوسط نفاذية عالية تصل إلى 87%، وانزياح في عتبة الامتصاص نحو الأطوال الموجية الطويلة. كما استخدمت هذه التقنية لحساب فجوة الطاقة للشرائح المحضرة، حيث لوحظ انخفاض قيمتها من3.44(eV) إلى3.28 (eV)، وزيادة في قيمة طاقة أورباخ من0.154(eV)إلى(eV) 0.186،

باختصار، أظهرت النتائج أن تطعيم أكسيد التيتانيوم بالليثيوم يؤدي إلى تحسين خصائص المادة وزيادة كفاءتها في التطبيقات المختلفة. كما أظهرت الشرائح المحضرة خصائص ضوئية، أما الكهربائية فتعذر علينا قياسها لشروط خصائص الشريحة المراد قياسها.

لخصت الدراسة إلى أن طريقة سائل هلام تعد تقنية فعالة لتطعيم أكسيد التيتانيوم بالليثيوم، وأن الشرائح المنتجة تمتلك خصائص فيزيائية وكيميائية تجعلها مناسبة للاستخدام في مجموعة واسعة من التطبيقات التقنية. توصي المذكرة بإجراء مزيد من الدراسات لاستكشاف إمكانيات تحسين خصائص هذه المواد وتطبيقاتها العملية.

الكلمات المفتاحية:أكسيد التيتانيوم, الأفلام الرقيقة، الطلاء بالدوران، التطعيم، الخصائص البنيوية، الخصائص الضوئية.

REPUBLIQUE ALGERIENNE DEMOCRATIQUE ET POPULAIRE
MINISTERE DE L'ENSEIGNEMENT SUPERIEUR
ET DE LA RECHERCHE SCIENTIFIQUE
UNIVERSITE MOHAMED KHIDER - BISKRA
Faculté des SE&SNV

الجمهورية الجزائرية الديمقراطية الشعبية
وزارة التعليم العالي والبحث العلمي
جامعة محمد خيضر بسكرة
كلية العلوم الدقيقة وعلوم الطبيعة والحياة

Département des Sciences de la matière

قسم :علوم المادة

Filière: Physique

شعبة :الفيزياء

تصريـــح شرفـــي

خاص بالالتزام بقواعد النزاهة العلمية لإنجاز بحث

(ملحق القرار 1082 المؤرخ في 2021/12/27)

أنا الممضي أسفله،

السيد(ة): ساريحي منال .....

الصفة: طالب سنة ثانية ماستر فيزياء تخصص: فيزياء المادة المكثفة

الحامل(ة) لبطاقة التعريف الوطنية رقم: 206749635 الصادرة بتاريخ: 2021/05/27

المسجل بكلية: علوم الطبيعة والحياة قسم: علوم المادة .....

والمكلف بانجاز أعمال بحث : مذكرة ماستر في الفيزياء

عنوانها: the effect of lithium doping on the properties of Titanium dioxide thin films elaborated by Sol-gel (spin coating)

أصرح بشرفي أني ألتزم بمراعاة المعايير العلمية والمنهجية ومعايير الأخلاقيات المهنية والنزاهة الأكاديمية المطلوبة في انجاز البحث المذكور أعلاه وفق ما ينص عليه القرار رقم 1082 المؤرخ في 2021/12/27 المحدد للقواعد المتعلقة بالوقاية من السرقة العلمية ومكافحتها.

التاريخ: 2024/05/30

إمضاء المعني بالأمر